

VILNIUS UNIVERSITY

RIMA BUDVYTYTE

**ARTIFICIAL PHOSPHOLIPIDS SYSTEMS FOR INVESTIGATIONS OF PROTEIN
AND PEPTIDE INTERACTIONS WITH BIOLOGICAL MEMBRANES**

Summary of doctoral dissertation
Physical sciences, biochemistry (04 P)

Vilnius, 2012

The research was carried out at the Department of Bioelectrochemistry and Biospectroscopy of the Institute of Biochemistry Vilnius University in the period of 2008 – 2012.

Scientific supervisor:

assoc. prof. dr. Gintaras Valinčius (Vilnius University Institute of Biochemistry, physical sciences, biochemistry – 04 P).

Consultant:

habil. dr. Gediminas Niaura (Center for Physical Science and Technology, physical sciences, chemistry – 03 P).

The thesis is defended at the Council of Biochemistry science direction of Vilnius University and Institute of Biochemistry:

Chairman – habil. dr. Valdemaras Razumas (Vilnius University, physical sciences, biochemistry – 04 P).

Members:

prof. dr. Rimantas Daugelavičius (Vytautas Magnus University, physical sciences, biochemistry – 04 P);

dr. Milda Plečkaitytė (Vilnius University, physical sciences, biochemistry – 04 P);

dr. Arvydas Skeberdis (Lithuanian University of Health Sciences, biomedical sciences, biophysics – 02 B);

dr. Vytautas Smirnovas (Vilnius University, physical sciences, biochemistry – 04 P).

Opponents:

prof. habil. dr. Albertas Malinauskas (Center for Physical Science and Technology, physical sciences, chemistry – 03 P);

dr. Rolandas Meškys (Vilnius University, physical sciences, biochemistry – 04 P).

The official discussion will be held at the public meeting of the Council of VU Biochemistry on October 19, 2012 11 a.m. in the hall of the Institute of Biochemistry.

Adress: Mokslininkų 12, Vilnius LT – 08662, Lithuania.

The summary of the thesis dissertation has been sent on September 19, 2012 m.

The dissertation is available at the Library of the Vilnius University and the library of VU Institute of Biochemistry.

VILNIAUS UNIVERSITETAS

RIMA BUDVYTYTĖ

**DIRBTINĖS FOSFOLIPIDINĖS SISTEMOS BALTYMŲ BEI PEPTIDŲ SAŲVEIKOS SU
BIOLOGINĖMIS MEMBRANOMIS TYRIMAMS**

Daktaro disertacija
Fiziniai mokslai, biochemija (04 P)

Vilnius, 2012

Disertacija rengta 2008 – 2012 metais Vilniaus universiteto Biochemijos instituto Bioelektrochemijos ir Biospektroskopijos skyriuje.

Mokslinis vadovas:

doc. dr. Gintaras Valinčius (Vilnius universiteto Biochemijos instituto, fiziniai mokslai, biochemija – 04 P).

Konsultantas:

habil. dr. Gediminas Niaura (Fizinių ir technologijos mokslų centras, fiziniai mokslai, chemija – 03 P).

Disertacija ginama Vilniaus universiteto ir Biochemijos instituto biochemijos mokslo krypties taryboje:

Pirmininkas – habil. dr. Valdemaras Razumas (Vilniaus universitetas, fiziniai mokslai, biochemija – 04 P).

Nariai:

prof. dr. Rimantas Daugelavičius (Vytauto Didžiojo universitetas, fiziniai mokslai, biochemija – 04 P);

dr. Milda Plečkaitytė (Vilniaus universitetas, fiziniai mokslai, biochemija – 04 P);

dr. Arvydas Skeberdis (Lietuvos sveikatos mokslų universitetas, biomedicinos mokslai, biofizika – 02 B);

dr. Vytautas Smirnovas (Vilniaus universitetas, fiziniai mokslai, biochemija – 04 P).

Oponentai:

prof. habil. dr. Albertas Malinauskas (Fizinių ir technologijos mokslų centras, fiziniai mokslai, chemija – 03 P);

dr. Rolandas Meškys (Vilniaus Universitetas, fiziniai mokslai, biochemija – 04 P).

Disertacija bus ginama viešame VU Biochemijos mokslo krypties tarybos posėdyje 2012 m. spalio mėn. 19 d. 11 val. Biochemijos instituto 522 kab. salėje.

Adresas: Mokslininkų 12, LT – 08862, Vilnius, Lietuva.

Disertacijos santrauka išsiuntinėta 2012 m. rugsėjo 19 d.

Disertaciją galima peržiūrėti ir Vilniaus universiteto ir VU Biochemijos instituto bibliotekose.

INTRODUCTION

Phospholipid membranes and proteins associated with them play an essential role in mediating the cell processes. However, the mechanisms of their function are not fully understood. Over the last decades, the investigation of protein functions and interactions within the cell membrane has been studied extensively. The tethered bilayer membranes (tBLMs), a new class of biomimetic models are a promising candidate as a stable and suitable platform for such studies. They provide excellent stability by covalently linking the bilayer membrane to a solid support. First designed by Vogel *et al.*, the inner leaflet of the membrane is bound to the solid support via a short spacer group¹. Such systems provide excellent electrical sealing, especially when phytanyl-based anchor lipids are used². Similar systems have been shown to allow for the functional incorporation of various membrane proteins^{3,4}. Planar surfaces, particularly if they are electrically conducting, are advantageous as they allow studies with many surface – sensitive techniques, some of them are used in this work, such as: atomic force microscopy and electrochemical impedance spectroscopy. In this dissertation design and development of tBLMs, also applications of these models for incorporation and detection of proteins (peptides) are described. The tBLMs will be analyzed by electrochemical impedance spectroscopy (EIS), fluorescence correlation spectroscopy (FCS) and fluorescence microscopy.

Pore – forming toxins (PFT), as the name suggests, disrupt the selective influx and efflux of ions across the plasma membrane by inserting a transmembrane pore. Ion channels, in general, play diverse roles in cells and organelles the transport of specific ions and macromolecules, conduction of signals and some of these are elements of cellular sensors. The protein **α -hemolysin** (α -HL) is a pore – forming toxin produced by the bacterium *Staphylococcus aureus*. The pathogenesis of *Staphylococcus aureus* is sepsis. It spontaneously self-assembles into a water soluble ionic channel with a molecular weight of 33.2 kDa and a length of ~ 10 nm. **Anthrax toxin** refers to three proteins secreted by virulent strains of the bacteria *Bacillus anthracis*. The pathogenesis of *Bacillus anthracis* depends on a secreted toxin that is believed to be responsible for the major symptoms of anthrax. The 63-kDa fragment of the protective antigen (PA63) component of anthrax toxin forms a heptameric channel, (PA63)₇ in acidic endosomal membranes that leads to the translocation of edema factor (EF) and lethal factor (LF) to the cytosol. The vaginolysin (VLY) – is cholesterol dependent cytolysin produced by *Gardnerella vaginalis*, resulting in the pathogenesis of bacterial vaginosis. The effect of PFT are directly related with interaction between toxin and phospholipid membrane. In this work, we demonstrate possibilities of EIS to detect toxins as well as to study interaction of toxins with artificial tethered bilayer membranes.

¹ H. Lang, C. Duschl, and H. Vogel, *Langmuir* 1994;(10):197-210.

² McGillivray D.J., Valincius G., Heinrich F., Robertson J.W.F., Vanderah D.J., Febo-Ayala W., Ignatjev I., Losche M., Kasianowicz J.J. *Biophysical Journal* 2009;96(4):1547-53.

³ Valincius G., Heinrich F., Budvytyte R., Vanderah D.J., McGillivray D.J., Sokolov Y., Hall J.E., Losche M. *Biophysical Journal* 2008; 95(10): 4845-61.

⁴ Ragure B., Braach-Maksvytis B., Cornell A.B., King G.L., Osman P.D.J., Pace R.J. Wiczorek L. *Langmuir* 1998;(14):648-59.

Alzheimer's disease (AD) is the progressive neurodegenerative disorder and the most common form of dementia in elderly. The central event in pathogenesis of AD is thought to be intracellular and extracellular accumulation of polypeptide compounds of low molecular mass – so called beta amyloid ($A\beta_{1-42}$) and their direct interaction with neural membrane. These molecules are tending to form supramolecular structures: nonsoluble fibrils, protofibrils and soluble oligomers. In this work, a propensity of amyloid oligomers to interact with an artificial phospholipid systems as well as to disrupt their integrity, was studied. For this study, various structural and spectroscopic techniques such as FCS, AFM, EIS, sum frequency generation (SFG) have been employed.

Aim of the dissertation:

The aim of this work is to design and characterize tethered bilayer lipid membranes (tBLM) mimicking cell membranes suitable for studying protein reconstitution and function in phospholipid environment. This work is interdisciplinary and brings together different fields of biochemical, biophysical and spectroscopic research to accomplish the objectives of the current work. From the biophysical viewpoint a complex study of protein – membrane interaction is taken to mean that investigation should be directed to following tasks:

- ✓ To design a biologically relevant tBLM suitable for studying effects of proteins (peptides) to membranes.
- ✓ To accomplish the reconstitution of pore forming toxins (α -hemolysin, anthrax toxin, vaginolysin) into the tBLM establishing the electrochemical features of the disruption of artificial phospholipid systems.
- ✓ To evaluate the functional and structural properties of $A\beta_{1-42}$ oligomers allowing to identify and characterized toxic variants of amyloid oligomers.
- ✓ To investigate the interaction of the soluble $A\beta_{1-42}$ with tBLM and to asses the mechanism of their damage to tethered membranes.

The scientific novelty and significance of the work:

Tethered lipid bilayer membranes (tBLMs) are complex molecular systems that open up a possibilities to be used it as experimental platform for the basic studies of the biomembrane structure and function. For the incorporation and study of proteins, ideal cell membrane models have to distinguish themselves by their stability, mobility of phospholipids and by a specific molecular architecture, which would allow to investigate them with surface-sensitive characterization techniques. That is why the main aim of this work is to design and characterize new solid supported tethered bilayer membrane (tBLM) systems, which will mimic a composition of neurons and other cells membranes.

In this, work a biomimetic tethered bilayer membranes were constructed using a special thiolipid compounds synthesized by our partner dr. D. Vanderah from the National Institute of Standards and Technology (NIST) at Gaithersburg, USA. This compound acts as an anchor that keeps phospholipid bilayer at the surface at a certain distance. We found the electrical properties and mobility of phospholipids in formed tBLM depend on the properties of these compounds. To mimic phospholipid environment in membranes physiological relevant composition of tBLM is required, so we developed a method for incorporating an important, not soluble in ethanol, lipid components. The modification is based on the direct exchange between the lipid vesicles and membrane. This technique, we believe, providing new avenues for the *in situ* modification of tBLM.

The impact of pore forming toxins is directly related to interactions between the cell membrane and a protein. The mode of interaction can vary between the specific or nonspecific. Thus, for the detection of toxins and the development of effective antitoxic products is important to have understanding about the molecular mechanism of the PFTs interaction with phospholipids. In this work, the tBLM interactions with PFT: α -HL, antrax toxin and a little known cholesterol dependent cytolysin – VLY, were studied and analysed by the EIS. In VLY case, the membrane damage was modulated by varying the amount of cholesterol in membrane. This allowed to reach limit of detection of this toxin as low as 5.8 nM, which is within the limits of detection by currently approved hemolytics tests.

Converging lines of investigation have revealed potential common cellular and molecular pathogenic mechanisms underlying many diverse neurodegenerative diseases such as Alzheimer, Parkinson, Huntington diseases and Amyotrophic lateral sclerosis. They include: abnormal protein dynamics with misfolding, defective degradation, proteasomal dysfunction and aggregation; oxidative stress (OS) and formation of free radicals/reactive oxygen species (ROS); impaired bioenergetics, mitochondrial dysfunctions and DNA damage⁵. There is a worldwide growing interest in AD research among scientists because of the huge medical and financial importance of the field, and the rapidly aging world population. However, the cellular and molecular mechanisms of AD are not well understood and a lot of questions are not answered. Which conformation and structure of aggregates are the most toxic? Why one form of amyloidic features are interacting with membranes and others no? Which structural differences of protein or phospholipids have influence in damage of neurons? What is the mechanism of disturbance of phospholipids membrane (dielectric, ionic, electrical or ligand-gated)?

Considering that, in this work, various kinds of molecular factors that affect oligomerization of $A\beta_{1-42}$ peptides were investigated. The structural and morphological features of $A\beta_{1-42}$ aggregates were evaluated by the surface sensitive (AFM, IR) and bulk (FCS, DLS, CD) techniques. The dependence of oligomer structure and properties on preparation protocol of $A\beta_{1-42}$ aggregates was observed. Hereby, the link between the size of the soluble $A\beta_{1-42}$ oligomers and their neurotoxicity was established. By the sum frequency generation spectroscopy we showed that both the $A\beta_{1-42}$ oligomers and fibrils are able to form surface-oriented absorption layers at air/water interphase, and to generate strong vibrational spectra. These SFG spectral “fingerprints”, may be used to discriminate the toxic amyloid oligomers from the non-toxic ones.

⁵ Jellinger K.A. *J Neural Transm* 2009; (116):1111–62.

In this work, the tBLMs were used as EIS-based sensor platform to detect both the dielectric damage and impairment of the insulating properties of the phospholipid membranes by the $A\beta_{1-42}$ oligomers. It was determined that the membrane damage mechanism by $A\beta_{1-42}$ oligomers may be different from the one of the forming toxins. We have established, that the $A\beta_{1-42}$ oligomers shows the high affinity to phospholipids membranes containing sphingomyelin. The important relation between size of aggregates, lipid composition of membrane and neurotoxicity, was documented by combining various biochemical, biophysical and spectroscopics techniques. In general, this research involved a broad spectrum of experimental methods, which were crucial in accomplishing aims of this dissertation.

Main statements for the defense of dissertation:

1. The nature of the molecular anchor used to immobilize the artificial membranes affects the geometry, the electrical properties, the lateral mobility of phospholipids, as well as their ability to functionally reconstitute proteins.
2. The defectiveness of tBLMs depends not only on the nature of an anchor but also on the nature of the immobilized phospholipids.
3. The lipid membrane extracts from cells can be immobilized onto the surface as functional tBLMs by the vesicle fusion.
4. The composition of tBLMs accomplished via rapid solvent exchange can be modified by an interaction with vesicles.
5. Insertion of cholesterol into tBLMs results in a decrease in the electric capacitance, activates the cholesterol dependent cytolysins and yield fluorescently visible domains on the surface of artificial membranes.
6. Pore forming toxins inserts into tBLM in a concentration-dependent manner, form water electrolyte-filled pores, in which an activation barrier of ionic mobility is close to that in the bulk solution.
7. The VLY cytolytic mechanism requires the presence of membrane cholesterol, but in the investigated artificial systems there is no needed for a CD59 receptor for the insertion of toxin and the initiation of the membrane damage.
8. *In vitro* $A\beta_{1-42}$ peptides tend to form aggregates with different morphology whereof the most neurotoxic forms are several nanometers soluble oligomers, which also strongly interact with tBLM.
9. Small toxic $A\beta_{1-42}$ oligomers exhibits higher affinity to the phospholipid bilayers compared to the non-toxic, though their secondary structures

estimated by circular dichroism and IR spectroscopies indicate no difference.

10. A β_{1-42} oligomers increase the dielectric constant of the membrane in tBLMs. This causes an ion migration barrier decrease and an increase of the membrane conductance.
11. Sphingomyelin enhances membrane damaging effect of A β_{1-42} oligomers in tBLMs. It decreases an activation barrier of amyloid-induced membrane conductance.

Dissertation contents:

The dissertation is written in Lithuanian and contains the following parts: Introduction, Literature review, Materials and Methods, Results and Discussion (3 Chapters), Conclusions, List of References (315 positions), List of Publications (3), Tables (14) and Figures (59). Total 199 pages.

MATERIALS AND METHODS

Materials for formation of tethered lipid membranes

H₂O was purified in a Millipore (Billerica, MA). Salts, buffers, organic solvents were obtained from Sigma-Aldrich, or FLUKA were of at least ACS reagent or analytical reagent grade.

Lipid anchor molecules: 20-tetradecyloxy-3,6,9,12,15,18,22-heptaohexatricontane-1-thiol (synthetic phosphocholine analog, WC14); 29-hexadecyloxy-3,6,9,12,15,18,21,24,27,31 dekaohaheptatetracontan-1-thiol (FC16); Z 20-(Z-octadec9-enyloxy)-3,6,9,12,15,18,22-heptaohatetracont-31-ene-1-thiol (HC18) – was synthesized by dr. D. J. Vanderah at National Institute of Standards and Technology, Gaithersburg, MD, USA.

Lipids: 1,2-diphytanoyl-*sn*-glycero-3-phosphocholine (**DPhPC**); 1,2-dioleoyl-*sn*-glycero-3-phosphatidilcholine (**DOPC**); 2-oleoyl-1-palmitoyl-*sn*-glycero-3-phosphocholine (**POPC**); 1-oleoyl-2-palmitoyl-*sn*-glycero-3-phosphocholine (**OPPC**); 1,2-Dieicozonoyl-*sn*-glycero-3-phosphocholine (**DEcoPC**); 1,2-dioleoyl-*sn*-glycero-3-phosphoethanolamine (**DOPE**); Cholesterol (**CHO**), Sphingomyelin (**SM**); Cerebroside (**CER**) (Avanti Polar Lipids, JAV); Lipid extracts from the rat cerebellum were kindly donated by colleagues from the Institute of Neuroscience at the Lithuanian University of Health Sciences.

Fluorescent lipids: 1,2-dioleoyl-*sn*-glycero-3-phosphoethanolamine-N-(lissamine rhodamine B sulfonyl) (ammonium salt) (**DOPE-LR**) Absorbance/Emission = 560/583 nm; 1,2-dioleoyl-*sn*-glycero-3-phosphoethanolamine-N-(7-nitro-2-1,3-benzoxadiazol-4-yl) (ammonium salt) (**DOPE-NDB**) – Absorbance/Emission = 460/535 nm; 25-[N-[(7-nitro-2-1,3-benzoxadiazol-4-yl)methyl]amino]-27-norcholesterol (**25-NBD CHO**) – Absorbance/Emission = 483/523 nm

Polyethyleneglycols (PEG) (Sigma Aldrich, Germany) – the following molecular mass PEG were used throughout the work: 100, 200, 400, 1000, 1500, 2000, 3400, 4000, 6000, 8000 or 10000. PEG were used as 15 % solutions in buffer.

Proteins and Peptides:

α -hemolysin (α -HL) from *Staphylococcus aureus* was purchased from Sigma Aldrich. **Anthrax toxin (PA₆₃)** – was a kind gift from Dr. John J. Kasianowicz (NIST, USA). **Vaginolysin (VLY)** – was donated by Dr. Aurelija Žvirblienė, from the Institute of Biotechnology, Vilnius University. Synthetic **Ab₁₋₄₂ peptide** (A β ₁₋₄₂) was from the American Peptide Company (California, USA). **HiLyte Fluor™ 555 labeled Ab₁₋₄₂** peptide was from Anaspec (California, USA).

Formation of tBLMs via rapid solvent exchange method

Si wafers (Silicon Quest Intl., Inc., Santa Clara, CA) were cleaned in two steps: gently wiping with Hellmanex solution (Hellma GmbH, M€ullheim, Germany) and immersion in Nochromix solution for 15 min. (Godax Laboratories, Inc., Cabin John, MD). Both steps were followed by rinsing with large amount of water. The cleaned wafers were coated with the Cr (10 Å) and Au (450 Å) films by the high energy magnetron sputtering (ATC Orion, AJA Intl. Inc., North Scituate, MA). Immediately after the sputtering, the coated wafers were used for the formation of anchor self-assembled monolayers (SAM). SAMs were produced by incubating freshly prepared gold surfaces in mixed solutions of WC14:ME, FC16:ME and HC18:ME, (ME denotes the β -mercaptoethanol) in ethanol at different molar ratios 3:7, 2:8, 8:2. Total concentration of thiols was 0.2 mM. The incubations was carried out for 12 – 18 h.

The rapid solvent exchange (RSE) technique first reported by Cornell et al. was used to complete the synthetic membrane. RSE also allows the formation of bilayers on SAMs of relatively low hydrophobicity, as is the case when a significant proportion of the hydrophilic backfiller ME is used⁶. tBLMs were completed by exposing the SAM-coated wafer to a 50 μ L of concentrated phospholipid solution (10 mM DOPC) in ethanol, followed by the rapid replacement of this solution by a large amount (approx..15 mL) of aqueous buffer (100 mM NaCl, 10 mM NaH₂PO₄, pH 7.4). The resulting molecular construct and its electric equivalent circuit are shown in Figure.1.

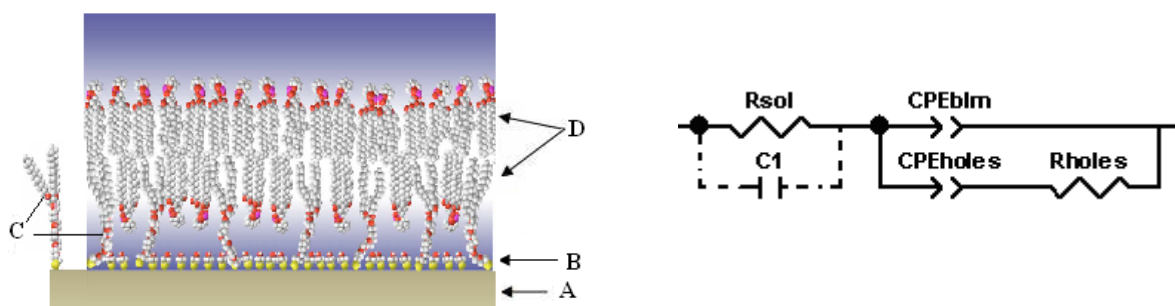


Figure 1. Molecular architecture of the tBLMs (left). A – Si/SiOx wafer coated gold; B – β -mercaptoethanol; C – Anchor molecules (WC14, FC16, HC18). Mixed SAM defines an ionic reservoir between the gold and the bilayer membrane; D – phospholipid that forms the bilayer membrane. An equivalent electrical model of the tBLM used, in this work, for the EIS data analysis.

Vesicle preparation

Vesicles were prepared by mixing the stock lipid solutions (10 mg/ ml) in chloroform at the various ratios, in a glass tube. 1 ml of lipid mixture was evaporated by a gentle stream of N₂. The residual solvent was removed by the vacuum-drying of the lipid film for 1 h. The film then was dissolved in pentane (1 ml) and left to dry overnight in the

⁶ McGillivray D.J., Valincius G., Vanderah D.J., Febo-Ayala W., Woodward J.T., Heinrich F., Kasianowicz J.J., Losche M. *Biointerphases* 2007;(2):21–33.

hood. The film was hydrated by adding 2.5 ml of the working buffer, 100 mM NaCl, NaH₂PO₄ (pH 7.4), sonicating for 60 min and incubating with occasional vortexing or until the lipid film at the bottom disappeared. The lipid preparation was then extruded (Avanti Polar Lipids, USA) through a 100 nm polycarbonate membrane for 21 times. Size distribution of vesicles was determined by the dynamic light scattering. The preparation exhibited a single peak centered on 150 nm. A large excess of vesicles was used in the oligomer binding to phospholipid experiments.

Preparation of A β ₁₋₄₂ oligomers and fibrils

Oligomers were generated as described by others.⁷ Briefly, soluble oligomers were prepared by dissolving 1 mg of peptide in 400 μ l HFIP for 30–60 min at room temperature. Sonication was used in this step. About 100 μ l of the resulting seedless solution was added to 900 μ l H₂O in a siliconized Eppendorf tube. After 10–20 min incubation at room temperature, the samples were centrifuged for 15 min at 12,000 rpm, the supernatant was transferred to a new siliconized tube and HFIP was evaporated. Concentration of HFIP in solution was monitored in FTIR spectra by a decrease in intensity of the 1192 cm⁻¹ band due to the asymmetric CF₃ stretching vibration⁸. Samples were incubated in closed vials for 24 h at 20 °C. This protocol is denoted as *protocol I*. To generate larger oligomers, typically 4–10 nm in diameter, the supernatant was transferred to a non-siliconized Eppendorf tube after the centrifugation and was gently purged with nitrogen for 7 min. The preparation was then stirred in the same vial at 500 rpm for 24 h using a magnetic Teflon coated stirring bar. Such a protocol will be further referred to as *protocol II*. Fibrils were formed by *protocol III* in which the aqueous peptide solution obtained after evaporation of HFIP was incubated for 7 days at room temperature.

*NaOH protocol*⁹: Preparation of HFIP – free A β ₁₋₄₂ oligomer samples using aqueous NaOH solution as a solvent. 0.3 mg A β ₁₋₄₂ were dissolved in 33 μ L of 100 mM NaOH at pH 12 and incubated for 25 min, followed by the addition of 800 μ L of 100mM NaCl, 10 mM NaH₂PO₄ buffer at pH 7.4-7.5 and were kept undisturbed at room temperature for 48 hours. Samples were store at 4 °C for later use.

Experimental methods

Characterization of A β ₁₋₄₂ oligomers and fibrils preparations

Atomic force microscopy (AFM)

To assess the size and morphology of the preparations of A β ₁₋₄₂ oligomers and fibrils, atomic force microscopy (Agilent 5500, Santa Clara, CA) was used in the tapping mode. Model TESP (Veeco, Plainview, NY) ($f = 257 - 301$ kHz, $k = 20 - 80$ N/m) and model PPPNCL - 20 ($f = 146 - 236$ kHz, $k = 21 - 98$ N/m) (Nanosensors, Neuchatel, Switzerland) microcantilevers were used in this work. According to the manufacturers,

⁷ Kaye R, Head E., Thomson J.L., McIntire T.M, Milton S.C., Cotman C.W., Glabe C.G. *Science* 2003;(300):486–9.

⁸ Czarnik-Matusiewicz B., Pilorz S, Bien D., Michalska D. *Vib. Spectrosc.* 2008;(47):44–52.

⁹ Lioudyn M.I., Broccio M., Sokolov Y., Rasool S., Wu J., Alkire M.T., Liu V., Kozak J.A., Dennison P.R., Glabe C.G., Losche M., Hall J.E.. *PLoS ONE* 2012;(7)4: e35090.

the probe tip diameters were between 16 and 20 nm. About 20 μl of a 10 μM $\text{A}\beta_{1-42}$ solution was spotted on freshly cleaved mica (SPI Supplies, West Chester, PA), incubated at room temperature for 10 min and rinsed with deionized water (Millipore Inc.), then blown dry with a nitrogen stream. Images were acquired at scan rates between 0.5 and 1 Hz with the drive amplitude and force kept to a minimum. The particle size was estimated by measuring the profile of the sample within the sample plane. The mean height of amyloid aggregates (“z-height”) was estimated by using the Plane Correction (Flattening) module of the SPIP software and determining step-height histograms.

Dynamic light scattering (DLS)

DLS experiments were performed on a Zetasizer Nano ZS (Malvern Instruments Ltd., UK) using a laser source with $\lambda = 633$ nm and a detector at a scattering angle of $\theta = 173^\circ$. Relaxation time distributions were obtained numerically from the field autocorrelation function $g(\tau)$ by means of a regularized inverse Laplace transform routine. Particle size distributions were extracted from the latter through the Stokes–Einstein equation: relation, $D = k_B T / (3\pi\eta d_h)$, between the diffusion constant D and the aggregate hydrodynamic diameter, d_h , and assuming spherical shapes of the particles.

Circular dichroism (CD)

$\text{A}\beta_{1-42}$ samples prepared using the methods described above were analysed by CD. CD spectra were collected on a Jasco J-810 spectropolarimeter. Spectra were obtained from 185 to 270 nm with a resolution of 0.2 nm and a bandwidth of 1 nm in a 1-cm path length quartz cell. Spectra were then converted to mean residue ellipticity and data were analyzed by using CDPro with algorithms: CONTIN, CDSSTR and SELCON3.

Sum frequency generation (SFG)

SFG spectroscopy were had used as surface and molecule specific tool to probe a $\text{A}\beta_{1-42}$ oligomers at air/water interface¹⁰. SFG spectra were recorded using EKSPLA (Vilnius, Lithuania) picosecond spectrometer. The spectrometer is based on a mode-locked Nd-YAG laser generating 25 ps pulses with 10 Hz repetition rate. The second harmonic radiation (wavelength 532 nm, pulse energy 200 – 300 μJ) from this laser was used as a visible beam. The tunable from 1000 to 3800 cm^{-1} infrared beam pulses with the energies of 80 to 200 μJ , respectively, were produced in the parametric generator OPD/DFG pumped by the third harmonic and fundamental radiation of the laser. The bandwidth of infrared beam was < 6 cm^{-1} . To produce vibrational sum frequency spectra the infrared and visible beams were incident at angles of 53° and 60° , respectively, and overlapped at the interface an area of 0.02 mm^2 . The signal was averaged over 50 – 100 pulses. SF spectra were normalized according to intensity of infrared beam to take into account the changes in radiation energy with wavelength. Spectra were collected in a glass cell which was 38 mm diameter. The cell was cleaned first with sodium hydroxide and subsequently with mixture of concentrated nitric and sulfuric acid solutions. After these procedures the cell was washed with ultrapure water. Before each set of experiments the clean less of the cell and aqueous phase was tested by recording the sum frequency

¹⁰ Niaura G., Budvytyte R., Kuprionis Z., Valincius G. *Proc. SPIE*, 2010;(7376):1-7.

generation spectrum of water. Absence of peaks in the C–H stretching region served as an indication that interface is sufficiently clean with respect to organic contaminants¹¹.

For a quantitative analysis of the sum frequency resonances, the experimental spectra have been fitted using the following expression¹²:

$$I_{SFG} \propto \left| \chi_{NR}^{(2)} + \sum_n \frac{A_n e^{i\psi_n}}{\omega_{IR} - \omega_n + i\Gamma_n} \right|^2, \quad (1)$$

where I_{SFG} is the sum frequency intensity, χ_{NR} is the non resonant contribution to the nonlinear susceptibility, ω_{IR} is the frequency of the incident infrared beam, and A_n , ψ_n , ω_n , and Γ_n are the strength, relative phase, resonant frequency and line width of the n th vibration, respectively. SFG measurements were conducted in a cylindrical glass cell with diameter 38 nm. Before experiments, the cell was cleaned with ammoniac persulfate solution in a concentrate sulfuric acid. After these procedures, the cell was washed with ultrapure (Milipore purified) water. The cleanness of the cell was studied aqueous phase was checked by SFG Spectroscopy. No peaks in the C-H stretching region were detected before adding the $A\beta_{1-42}$ oligomers, which it indicated absence of organic contaminations at studied solution/air interface. Polarization-dependent experiments provide possibility to determine the orientation of particular molecular groups. Normal to surface components of vibrational transition moments are probed by ssp polarization combination, while parallel components are probed in sps spectra. Both, normal and parallel components contribute to ppp spectra.

The SFG experiments were carried out in collaboration with Habil. dr. G. Niaura and Dr. Z. Kuprionis (EKSPLA, Vilnius), while the spectral data analysis and interpretation was done by Dr. G. Niaura.

FTIR

FTIR measurements were performed on a Perkin-Elmer model Spectrum GX FTIR spectrometer equipped with a DTGS detector. FTIR spectra were recorded in transmission mode. The spectral resolution was set to 2 cm⁻¹ and spectra were acquired by co-addin 50 scans. HFIP solution spectra were recorded in a sealed cell with 25 lm path length equipped with CaF₂ windows. $A\beta_{1-42}$ preparations were deposited on CaF₂ substrate from 60 l M solution and were dried in air. The spectral data analysis and interpretation was done by Dr. G. Niaura.

Characterization of tBLM and study of their interaction with proteins

Electrochemical impedance spectroscopy (EIS)

EIS was performed with a Solartron 1287A and a Parstat 2273 (Princeton Applied Research, TN) potentiostat and a 1260 frequency analyzer (Farnborough, UK). Au-coated silicon wafers (20 × 40 mm) served as the working electrode. For EIS

¹¹ Niaura G., Kuprionis Z. Suminio daznio generacija. Vilnius 2009: 153-84.

¹² Vidal F. and Tadjeddine A. *Rep. Prog. Phys.* 2005;(68):1095–27.

measurements six separate electrochemical cells (250 – 300 μL volume each) located on the same wafer were with working area of 0.32 cm^2 of the gold film exposed to the solution. A saturated silver-silver chloride [AgAgClNaCl_{aq,sat}] microelectrode (Microelectrodes, Bedford, NH, model M-401F) was used as a reference. The auxiliary electrode was a 0.25 mm diameter platinum wire (99.99% purity, Aldrich) coiled around the barrel of the reference electrode. The distance between the tip of the reference and working gold electrode surface was set to 2 – 3 mm. All measurements were carried out at 0 V bias versus the reference electrode at $21 \pm 1^\circ\text{C}$ in aerated solutions. EIS spectra were normalized to the geometric surface area. EIS curves were fitted to an equivalent circuit model shown in Fig.1 using ZView software (Scribner Associates, Southern Pines, NC).

Fluorescence microscopy (FM).

Investigation of optical homogeneity of tBLM was done by the Fluorescence microscopy. FM was performed on commercial Zeiss microscopes (Carl Zeiss, Jena, Germany): an Axiovert 100 epifluorescence microscope fitted with an EM-CCD mod. C9100 video camera (Hamamatsu Photonics, Herrsching, Germany). On the Axiovert 100, a Zeiss filter set (excitation: BP 510–560, beam splitter: FT 580, emission: LP 590) was used to image the lateral distribution of LR-DOPE through a Zeiss Water Achroplan (20_0.5 NA) objective lens. For FM measurements the rapid solvent exchange and vesicle fusion was performed by introducing the 5 x5 mm^2 splinters into the Nunc Lab-Tek chambered cover glass (Thermo Fisher Sci., Rochester, NY) sample cell, where they rested without fixation. Phospholipids were doped with 0.06 mol % with LR-DOPE for FM experiments,

Fluorescence Correlation Spectroscopy.

The investigations of the diffusivity of phospholipids in tethered bilayers, prepared using high and low density of self assemble monolayer were analysed by FCS. tBLMs were prepared with 5×10^{-3} mol% LR-DOPE admixed to the DOPC solutions. The two-photon FCS system consists of a Verdi 10 W continuous wave DPSS laser ($\lambda = 532 \text{ nm}$) that pumps a Mira 900F mode-locked titanium-sapphire laser (125 fs pulse-width, 76 MHz repetition rate, 1.8 W at $\lambda = 780 \text{ nm}$) from Coherent (Santa Clara, CA). The output wavelength from the Ti-sapphire laser can be tuned between 700 nm and 980 nm, and $\lambda = 840 \text{ nm}$ is used for exciting lissamine-rhodamine labeled lipids. A neutral density (ND) filter attenuates the IR output to 5 – 10 mW before it enters the reflector turret of an Axiovert 200M inverted microscope (Carl Zeiss, Jena, Germany). The light then passes through a dichroic mirror (750 dexpxr; Chroma Technologies, Rockingham, VT) and is focused using a $63 \times 1.2 \text{ NA}$ C-Apochromat water immersion lens (Carl Zeiss) corrected for the coverslip thickness (0.14 – 0.18 mm). The fluorescence is epifluorescence collected, passed through a bandpass filter (et575/50m-2p, Chroma Technologies), focused via the microscope tube lens, re-collimated via an achromatically corrected doublet lens, split into two beams with a 50:50 beam splitter cube (Thorlabs, NJ) and focused via two achromatically corrected doublet lenses onto two separate avalanche photodiode detectors (SPCM-AQR14, Perkin-Elmer, Fremont, CA).

For a quantitative analysis of the fluorescence autocorrelations, the experimental spectra have been fitted using the following expression for one freely diffusing species of molecules (3D model¹³):

$$G(\tau) = \frac{1}{V_{\text{eff}} \langle C \rangle} \cdot \frac{1}{\left(1 + \frac{\tau}{\tau_D}\right)} \cdot \frac{1}{\sqrt{1 + \left(\frac{r_0}{z_0}\right)^2 \cdot \frac{\tau}{\tau_D}}} \quad , \quad (2) \quad \tau_D = \frac{r_0^2}{\alpha \cdot D} \quad (3)$$

The first factor in Equation 2 is exactly the inverse of the average particle number in the focal volume. V_{eff} – effective focal volume. The 1/e² radius is given by r_0 in lateral direction, whereas it is z_0 in the axial direction. The lateral diffusion time τ_D that a molecule stays in the focal volume can be expressed in terms of the diffusion coefficient D (equation). Where α is 8 for two photon excitation PE. The autocorrelation function for two-dimensional diffusion, for example, in a membrane reads:

$$G_{2D}(\tau) = \frac{1}{N} \cdot \frac{1}{1 + \frac{\tau}{\tau_D}} \quad , \quad (4)$$

FCS data were fitted with a 3D diffusion model (equation 2) providing the $A\beta_{1-42}$ oligomers diffusion coefficient, which converts into oligomer size via the Stokes–Einstein equation. Concerning corrections for nonspherical aggregate shapes. Also for $A\beta_{1-42}$ oligomers interaction with phospholipids membranes (vesicles), FCS data were analyzed with 3D diffusion model with two components (one – autocorrelation of $A\beta_{1-42}$ oligomers, second autocorrelation of $A\beta_{1-42}$ oligomers with bind vesicles).

The FCS measurements were performed at Carnegie Mellon University, Pittsburgh, PA, USA in collaboration with prof. Mathias Losche group.

¹³ Hausteil E., Schwille P., *Annu. Rev. Biophys. Biomol. Struct.* 2007; (36) :151–69.

Chapter I. Artificial tethered phospholipids membranes: development and characterization

1. EIS characterization of tBLMs

The typical EIS spectrum of the formation process of phospholipid bilayer membrane and its electrical parameters is shown in Fig. I.2. The spectra are presented in the Cole-Cole complex capacitance format (imaginary, C'' vs. real, C' complex capacitance component plot), which is very convenient for studying such a systems (Figure I.2.). It exhibited a semicircular shape, consistent with the capacitive behavior of a near ideally insulating dielectric layer and it is proportional to electrical capacitance of the layer. Changes in the EI spectra upon tBLM completion were consistent with a thickness increase of the dielectric layer. In particular, the semicircular diameter in the Cole-Cole plot, proportional to the layer capacitance, shrunk by a factor of ≈ 10 , as we can see in Figure 2, from ~ 7 to $0.76 \mu\text{F}/\text{cm}^2$.

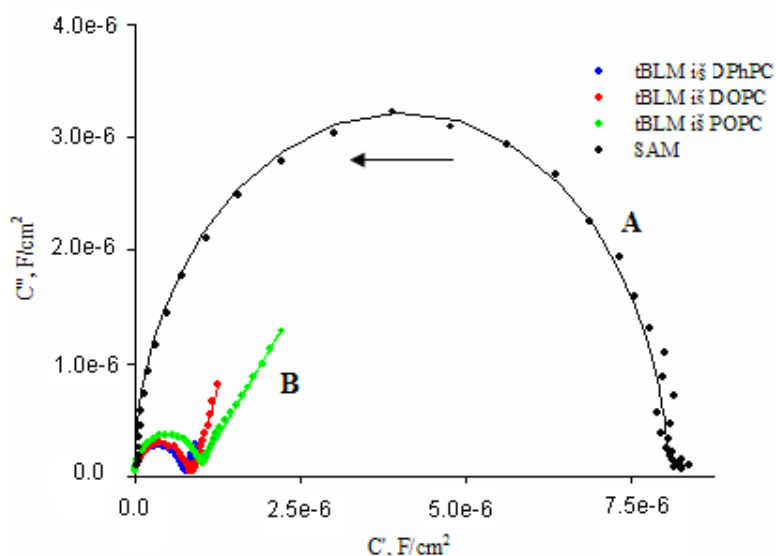


Figure I.2. The complex capacitances changes of self assembly monolayer and tBLM. A. Cole-Cole, capacitance plots of EIS spectra, normalized to A_{el} , of SAMs (β -ME : WC14 = 7:3). B. The capacitance plots of tBLMs (β -ME:WC14 = 7:3 + phospholipid) completed with: blue - DPhyPC; red - DOPC, green - POPC. An arrow shows the increasing direction of frequency. The frequency range of EIS spectra is from 0.5 to 10^5 Hz. Parameters are normalized to a geometric surface area.

EIS spectrum of molecular anchor layer was fitted to a simple series equivalent circuit, CPE-R, that is widely used for modeling dielectric properties of single component alkanethiol SAMs (Fig. I.2, A). Whereas the EIS spectra of tBLM differ

form the one of the SAMs not only quantitatively but also qualitatively. Typically, in tBLM EIS a new feature appeared in the form of a low frequency “tail” that frequently was a straight line and of considerable variability in length for different samples. These low frequency tails cannot be adequately described by the simple equivalent circuit used for the SAM. However, the equivalent circuit model represented in Fig. 1, which accounts for membrane defects, described all features quite well. Despite these additional features, the EI spectra exhibited near ideal capacitive behavior in the high frequency range (small semicircle) with modeled CPE_{tBLM} exponent values, α_{tBLM} , of 0.99, indicating near ideal capacitive behavior of phospholipid bilayers. The low frequency tails attributed observed in the tBLM systems were attributed to the intrinsic defectiveness of tBLMs (Fig. I.2 B). So, the resistance R_{def} , reflected the extent of the defectiveness. Similarly, the CPE_{def} in Fig.1 reflects the electrical conductivity of the submembrane space, however, it is also dependent on the defectiveness. Typically, at low defect density, the CPE_{def} exponent was found to be close to $\alpha_{def} = 0.5$; while the increasing defect density, lead to a shift of the exponent towards $\alpha_{def} \rightarrow 1$.

To compare the propensity of different phospholipids to form tBLMs a series of RSE experiments with DPhPC, DOPC, POPC, OPPC and EcoPC were carried out. The properties of the resulting tBLMs were tested by an EIS. Fitted to a model parameters are summarized in Table I. The capacitance values (less or about $1 \mu F/cm^2$ attest for the formation of tBLMs in all cases. However, the defectiveness of tBLMs is different. In the sequence DPhPC, DOPC, DEcoPC, POPC, OPPC the R_{def} decreases from 1180 to $0.72 k\Omega \cdot cm^2$, while the exponent of the CPE_{def} increases from ≈ 0.5 to ≈ 1 . Both trends attests for the increasing defectiveness of the tBLMs, suggesting it to be affected by the nature of the phospholipid used to accomplish the tBLM via RSE.

Table I. Best – fit parameters (model in Figure 1) of the EI spectra of tBLMs of various compositions formed WC14/ME based SAMs. The values of parameters are normalized to a geometric surface area, A_{el} .

<i>Parameters</i>	<i>Phospholipids</i>				
	DPhPC	DOPC	EcoPC	POPC	OPPC
$CPE_{tBLM}, \mu F/cm^2$	0.79	0.85	0.93	1.10	1.18
α_{BLM}	0.982	0.979	0.975	0.951	0.906
$CPE_{def}, \mu F/cm^2$	4.72	5.78	6.25	8.81	8.84
α_{def}	0.549	0.649	0.662	0.928	0.947
$R_{def}, k\Omega \cdot cm^2$	1180	620	136	6.17	0.72
Fit quality parameter, $\chi^2 \times 10^4$	2.41	4.67	2.56	1.43	4.78

2. The influence of anchor molecules to properties of tBLM

The assembling strategies of tBLM are mostly depend on the spacer molecules and the type of anchor or layers and the nature of the substrate¹⁴. Densely packed tether lipids at the surface (no backfilling with β ME) typically lead to very high membrane

¹⁴ Junghans A. and Koper I. *Langmuir* 2010; 26(13):11035–40.

resistances, however this can be a problem to the functional reconstitution of protein¹⁵. The choice of the bilayer construction strategy is influenced by the surface technique which have to be used for characterization and by the substrate properties that are required for analyses.

By now, our group in collaboration with dr. D.Vanderah (NIST, USA) and prof. M. Losche groups (Carnegie Mellon University, USA) have been developed tBLMs with several anchor lipids: WC14, FC16 and HC18. In the current work, a comparative study of structural and functional properties of tBLMs based on these molecular anchors is presented. The saturated FC16 anchor has longer polymethylene chains and a nonaethyleneoxide tether compared to WC14 (dimyristyl and six ethylene oxide units),¹⁶ whereas HC18 contains double bond in each of the hydrophobic chains, and a hexaethylene oxide linker.

Figure I.3 compares EIS results of HC18 SAMs with those of its saturated analogs WC14 and FC16. As seen in Fig. I.3 A, all SAMs exhibit nearly perfect semicircular Cole – Cole plots at low tether molecule ratios, *e.g.*, 30%, with HC18 consistently exhibiting lower capacitance values. Also, the exponent of the constant phase element (CPE), shows consistently higher values for HC18 than for WC14 and FC16 (Table II). At higher molecular ratios, *e.g.*, 70 % (Fig. I.3 B), the EIS spectra of HC18 SAMs differ drastically from those of WC14 and FC16. While the latter compounds produce compact low capacitance SAMs with capacitances of $\sim 1 \mu\text{F}/\text{cm}^2$, HC18 produced SAMs with about six-fold higher capacitances at molecular ratios 70 %.

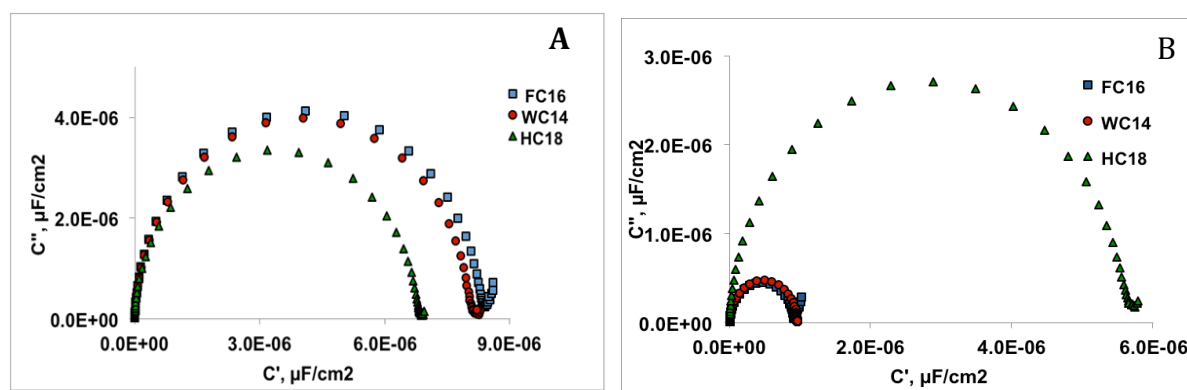


Figure I.3. Cole – Cole plots of electrochemical impedance spectra of HC18 (Triangles), WC14 (circles) and FC16 (squares) SAMs at different anchor/backfiller ratios: A) 30:70; B) 70:30. The capacitance plots of EIS spectra are normalized to A_e .

Upon membrane formation by rapid solvent exchange all SAMs at low tether molecule ratios, 30 %, shows spectral changes in EIS commensurate with the formation of insulating phospholipid bilayer. In all cases, the capacitance of tBLM decreases by a factor of ≈ 10 (Table II). Such capacitance values would be expected if the dielectric layer has the thickness of about 3 nm and the relative dielectric constant from 2 to 3. At high tether molar ratio, at 70 %, EIS such large spectral changes upon phospholipid addition are seen only in HC18 case, while the formation of phospholipid layer on SAMs

¹⁵ Glazier A.S., Vanderah J.D., Plant L.A., Bayley H., Valinčius G. And Kasianowicz J.J. *Langmuir*. 2000;(16):10428-35.

¹⁶Heinrich F., Ng T., Vanderah D.J., Shekhar P., Mihailescu M., Nanda H. and Losche M. *Langmuir* 2009;(25):4219-29.

of WC14 and FC16, triggers only a slight decrease of capacitance (Table II). Such a case is consistent of the addition just one leaflet of the phospholipid forming a structure known as a hybrid bilayer. So, we may resume that the nature of anchor molecule affects the electric parameters an anchor SAM. The formation of tBLMs can be monitored by the capacitance changes.

Table II. Equivalent circuit EIS model fits of various SAMs and prepared DOPC tBLMs by rapid solvent exchange of various tether compositions and backfiller (β ME) ratios.

<i>Anchor compound</i>	$CPE_{SAM}, \mu F/cm^2$	α_{SAM}	$CPE_{tBLM}, \mu F/cm^2$	α_{tBLM}
	<i>SAM</i>		<i>tBLM, DOPC</i>	
<i>WC14 30%</i>	8.61 ± 0.544	0.9864 ± 0.009	0.89 ± 0.075	0.9867 ± 0.003
<i>FC16 30%</i>	8.90 ± 0.290	0.9882 ± 0.003	0.87 ± 0.045	0.9818 ± 0.002
<i>HC18 30%</i>	6.92 ± 0.047	0.992 ± 0.002	0.84 ± 0.016	0.9909 ± 0.002
<i>WC14 70%</i>	1.00 ± 0.032	0.9958 ± 0.002	0.65 ± 0.007	0.9984 ± 0.001
<i>FC16 70%</i>	0.93 ± 0.014	0.9931 ± 0.005	0.62 ± 0.024	0.9970 ± 0.001
<i>HC18 70%</i>	5.89 ± 0.164	0.9934 ± 0.002	0.80 ± 0.047	0.9952 ± 0.002

1. Diffusivity of phospholipids in tethered bilayers

Different anchors result in different structure and physical properties of tBLMs. One of such properties is lateral lipid mobility. To test if the phospholipid mobility is dependent on the nature of the molecular anchor we measured 2D FCS using tBLMs accomplished on HC18, WC14 and FC16. DOPC was chosen as a test phospholipid. Data is summarized in Table III.

Data indicate that both on low and high anchor density, the lateral mobility of phospholipid is noticeably higher on unsaturated HC18 tethered tBLMs. Saturated analogs exhibited at least two-fold lower phospholipid mobility. This result shows an increased mobility, an presumably flexibility of phospholipid tBLMs accomplished on unsaturated SAMs pointing out to possible advantage of HC18-based tBLMs as a matrix for the reconstitution of proteins and peptides, as demonstrated further.

Table III. Lipid diffusivities in densely packed tBLMs.

Anchor	2D Diffusion coefficient $D, \mu m^2/s$
HC18 70%	$4.03 \pm 0.21 (n = 6)$
FC16 70%	$1.6 \pm 0.16 (n = 5)$
WC14 70%	$1.9 \pm 0.18 (n = 6)$
HC18_ 30%	$6.2 \pm 0.46 (n=7)$
FC16 30%*	4.1 ± 0.1
WC14 30%*	3.6 ± 0.2

* Siddharth Shenoy, et. al., 2010.

4. tBLM modification by vesicles fusion

tBLMs prepared by rapid solvent exchange, leads to highly insulating bilayer but provides limited control over membrane composition. Typical tBLM techniques have limited possibilities of producing asymmetrics or multicomponents bilayers. However, incorporation of a wide range of membrane components, including membrane proteins, and other lipids poses formidable technological challenge. To change their composition we suggest applying method of direct lipid exchange between the vesicles and membranes¹⁷.

Cholesterol effect on the capacitance of tBLMs

To assess the extent of cholesterol transfer from vesicles to tBLMs we first accomplished cholesterol contained tBLMs through the rapid solvent exchange using a methanol as an exchangeable solvent. The introduction of cholesterol triggers obvious changes in EIS curves. In particular, the semicircular part of the curve shrinks, which is indicative of the tBLM capacitance decrease. Fitting to a model allowed us to build the capacitance versus cholesterol concentration plot, which is shown in Fig. I.4 B.

One of the most striking features of the plot in Fig. I.4 is an almost linear decrease tBLM capacitance with cholesterol concentration. There are several reasons that may be responsible for the capacitance decrease in tBLM systems, however, the discussion of this issue is beyond the scope of the current work. We note here, that the decrease of the capacitance may serve as an indicator of the cholesterol transfer from the vesicles if such occur in the systems under the study.

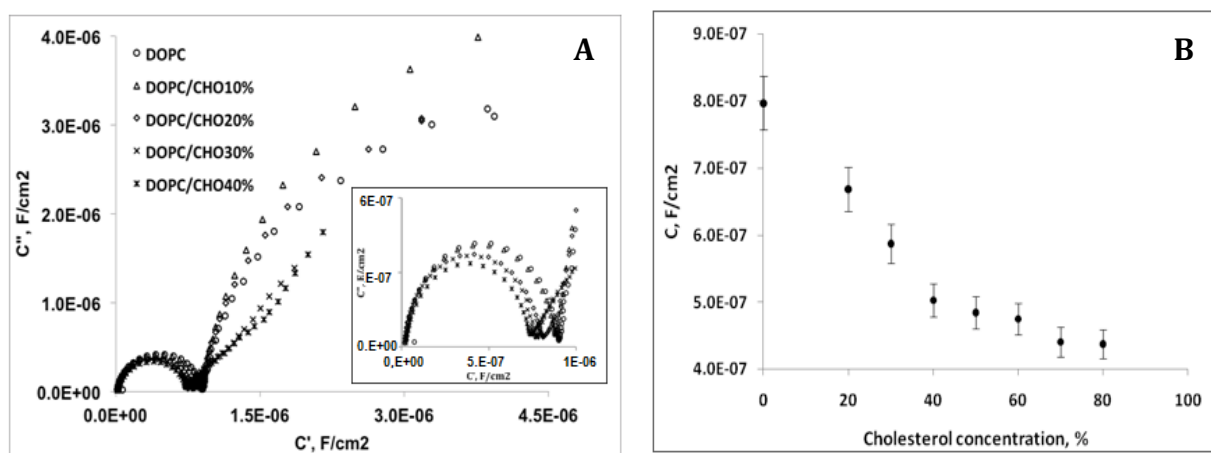


Figure I.4 A. Cole-Cole plots of electrochemical impedance spectra of tBLM completed with DOPC and prepared on the precursor SAM: FC16:ME (3:7 mol:mol in 0.1 M NaCl, pH 7.4) as a function of cholesterol concentration for: no cholesterol (circles); 10 % cholesterol (triangles); 20 % cholesterol (diamond); 30 % cholesterol (stars); 40 % cholesterol (criss-cross). **(Inset)** An expanded view. The data were normalized with respect to the geometric surface area (A_{el}).

I.4 B. Effect of cholesterol on membrane capacitance of tBLM (FC16:bME 3:7, DOPC/DOPE; in 0.1 M NaCl, pH 7.4) as a function of cholesterol concentration.

¹⁷ Kunze A., Svedhem S., and. Kasemoet B. Langmuir, 2008;(25): 5146-58.

Cholesterol donor vesicles triggers changes of the capacitance of tBLMs

To test if the cholesterol is transferred from the vesicles to the tBLMs, the latter were exposed to DOPC vesicles containing 30% of cholesterol. Figure I.5 A shows that after 60 min of exposure to the vesicle solution the semicircular part of the EIS curve of pure DOPC tBLM (filled circles) shrinks (open triangles), and it approaches the curve (positive control, open diamonds) obtained by introducing the cholesterol at 30% by the rapid solvent exchange. The negative control experiment is shown in Fig I.5 B. Under the same conditions, the tBLM was exposed to the cholesterol-free DOPC vesicles. Barely noticeable, marginal variation of the diameter of the EIS curve can be seen in this case.

Table IV summarizes the fitted to a model tBLM capacitance data. Because the exponent of the CPE_{tBLM} in all systems is close to 1, we may assume the following $CPE_{\text{tBLM}} \approx C_{\text{tBLM}}$, where C_{tBLM} is the capacitance of the dielectric barrier formed by the phospholipid bilayer. Data in Table IV shows a significant reduction of the capacitance of DOPC tBLMs upon exposure to cholesterol donor vesicles, while noticeably smaller variation is seen for the cholesterol-free vesicles. We note that in addition to the capacitance decrease, the CPE exponent shift towards 1 is visible in the fitted data. Typically, we observed higher α_{CPE} values for cholesterol-containing tBLMs. This may be related to a “condensing effect” of cholesterol on the membrane phospholipids known from the structural studies.

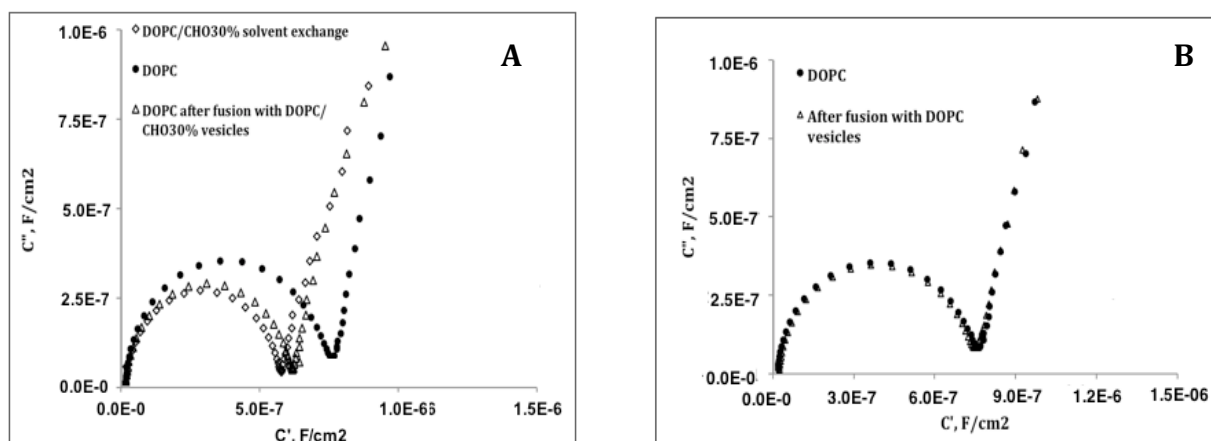


Figure I.5. Cole – Cole plots of electrochemical impedance spectra of tBLMs prepared on the precursor SAMs: HC18:ME (3:7 mol:mol in 0.1 M NaCl, pH 7.4) and completed: (A) with DOPC/CHO30% by rapid solvent exchange (Diamonds); with DOPC by rapid solvent exchange (Circles) with DOPC after modification by fusing DOPC/CHO30% vesicles (Triangles); (B) with DOPC by rapid solvent exchange (circles); with DOPC after modification by fusing DOPC vesicles (Triangles).

Table IV. Best – fit parameter (model in Figure 1) to electrochemical impedance spectra of CPE_{tBLM} of tBLMs from Fig.7 before and after modification by vesicles fusion. The values of tBLM completed with DOPC/CHO30% by rapid solvent exchange are correlate with results by vesicle fusion The values of parameters are normalized to A_{el} .

<i>EIS parameters</i>	<i>tBLM</i>	<i>After modification by vesicle fusion</i>	<i>By rapid solvent exchange</i>
	DOPC	DOPC	
$CPE, \mu F/cm^2$	0.84 ± 0.02	0.81 ± 0.03	
α_{tBLM}	0.976	0.975	
	DOPC	DOPC/CHOL30	DOPC/CHOL30
$CPE, \mu F/cm^2$	0.84 ± 0.02	0.69 ± 0.01	0.61 ± 0.02
α_{tBLM}	0.976	0.990	0.990

Fluorescence microscopic evidence of lipid and cholesterol transfer from vesicles to tBLMs

The EIS indirectly, through the capacitance decrease, attests for the cholesterol transfer from vesicles to tBLMs. So far, it has limited ability to test the transfer of phospholipids in a similar manner. The direct evidence of the transfer of both phospholipids and cholesterol may be demonstrated by using the fluorescence microscopy (FM). The invisible to a FM pure DOPC tBLM was exposed for 60 min to cholesterol-containing vesicles that, in addition, were fluorescently labeled with two markers: LR-DOPE, and CHO- NDB (both at 0.05% level). Fig. I.6 shows the FM images obtained from the same patch of tBLM with different color filters for correspondingly LR (yellow) and NDB (green) fluorophores. From Fig. I.6 it follows that the exposure of the tBLM to vesicles resulted in transfer of both the phospholipids (DOPE, and presumably, DOPC) and the cholesterol.

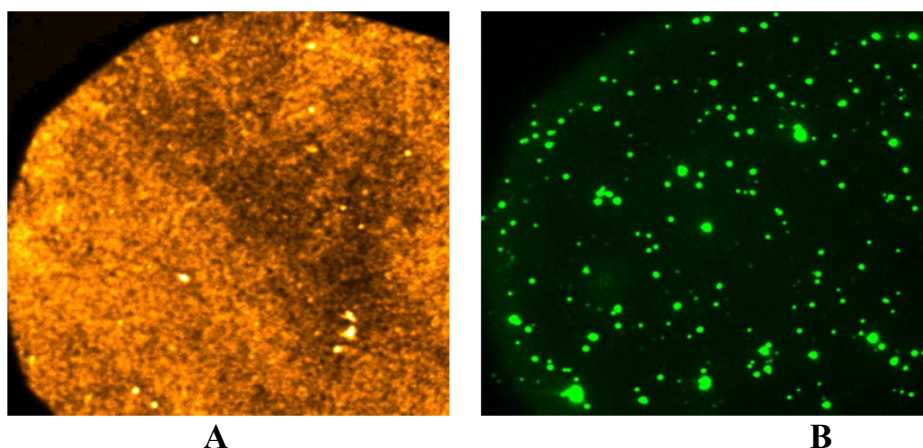


Figure I.6. Simultaneous transfer of lipid material from donor DOPC/CHO30% vesicles with LR-DOPE and also with NDB-CHO labeled, with concentration is 0.05 mol%, to the DOPC tBLM. The contrast in the original image has been linearly enhanced. Fluorescence micrographs of tBLM after fusion of vesicles **A.** DOPC transfer. **B.** Cholesterol transfer. Objective 50X, the diameter of the image: 120 μ m.

Notably, the phospholipids are transferred to a membrane in a highly homogeneous manner, while the cholesterol yields the fluorescently visible micrometer-size domains on the surface of the artificial membrane. In addition to an EIS experiment, this confirms the possibility of modification compositions of tBLMs by the material exchange with vesicles.

5. Multicomponent tethered bilayers

In this work, we attempted mimicking natural membrane compositions by two different approaches. First is based on the preparation of complex phospholipid mixtures from the synthetic components. Second is based of the ability of certain anchor molecules to fuse vesicles made of natural lipid extracts.

tBLMs that mimic the composition of neuronal membranes

To assemble artificial membranes that mimic neuronal membranes we used the following, physiologically relevant molar ratios of synthetic phospholipids¹⁸: [PE]/[PC] = 0.3; [CHO]/[phospholipids] = 0.36; [SM]/[total lipids] = 0.05, [CS]/[total lipids] = 0.03. Because not all of these lipids are soluble in ethanol we developed a protocol based on a methanol as an exchangeable solvent. The new protocol allowed obtaining well-insulating and stable tethered bilayers containing up to a five components in the bilayer. The homogeneity of the bilayer was tested by FM. Fig. I.7 A displays the FM image of a five-component tBLM fluorescently labeled with 0.05 mol % LR-DOPE. The FM image, typically showed some dark spots on the surface of tBLMs, attesting for the inhomogeneities in tBLMs.

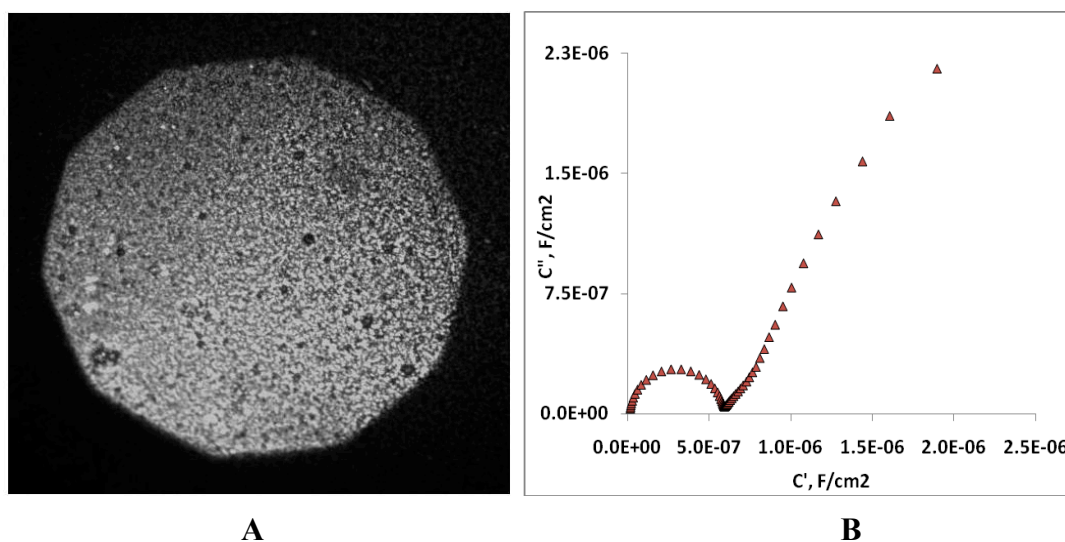


Figure I.7. The fluorescence image and EIS spectra of multicomponent tBLM. **A.** Fluorescence micrographs of tBLM based upon FC16/bME (30:70) and (DOPC/DOPE/SM/CHO/Cer) with labeled LR-DOPE in lipid mixture. Objective 20X, the seeing diameter of view: 250 μ m. **B.** Cole-Cole plots of electrochemical impedance spectra of multicomponents tBLMs. The data are normalized to the geometric surface area (A_{el}). The frequency range is from 0,1 to. 10⁵ Hz.

¹⁸ Hamberger A. and Svennerholm L. *J Neurochem.*1971;(18):1821-9.

This may be either incomplete surface patches without phospholipid bilayer, or patches containing fewer or no fluorescent label. To verify the completeness of the five-component bilayer we carried out the EIS test, shown in Fig. I.7. The EIS curve indicates almost perfect semicircular patch at the beginning of the plot (high frequency range), and an extended low frequency tail, that starts with short almost 45° slope stretch, which, according to recently published mathematical analysis¹⁹ should appear in EIS spectra when low density large, micrometer size defects are present. Consequently, FM and EIS indicate a complete bilayer is accomplished via RSE. However, they are populated by scattered, low density both large, over a micrometer size, and small not visible in FM, but detectable by the EIS, defects.

The fusion of vesicles, prepared from lipid extract of rat neuron membrane

The vesicles from lipids extracts from rat cerebellum membrane were used in this work had a diffusion coefficient $24.74 \pm 2.02 \mu\text{m}^2/\text{s}$. So, the dynamic radius of the vesicles was $87 \pm 8 \text{ nm}$. It was smaller than that of the vesicles prepared from the synthetic lipids under the same conditions. Fusion of pure lipid bilayers and biological membranes is strongly modulated by lipid additives that alter membrane curvature²⁰. So it was not clear whether and how such vesicles will fuse to the molecular anchor utilized for the design of tBLMs in current work.

For the vesicle fusion experiment the 70 % HC18 SAM was chosen. From our data it was clear that such SAM having enough hydrophobicity necessary for vesicle fusion retains high lateral mobility of phospholipids, which is important in the formation of a functional model membrane.

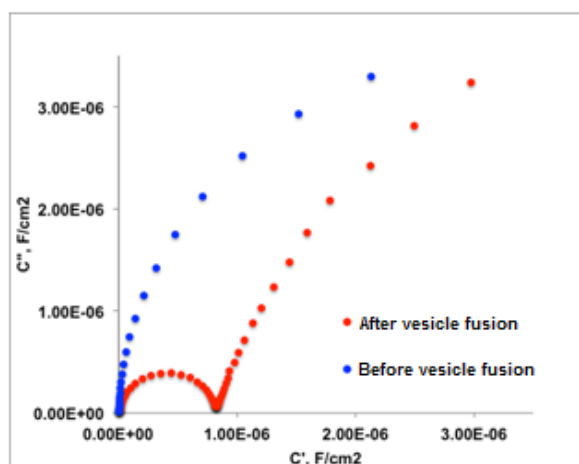


Figure I.8. Cole-Cole plots of electrochemical impedance spectra of tBLMs prepared on the precursor SAMs (blue): HC18:ME (3:7 mol:mol in 0.1 M NaCl, pH 7.4) and completed by fusing a real lipid neuron membrane extract vesicles (red).

A figure I.8 shows the Cole Cole plots of the spectra of SAM (blue circles) and tBLM completed by fusing vesicles prepared from lipid extracts of rat cerebellum (red circles) and Table V summarizes the electrical parameters of fusion calculated from such

¹⁹ Valincius G., Meskauskas T., and Ivanauskas F. *Langmuir* . 2012;(28):977-90.

²⁰ Chernomordik L., Kozlov M.M., Zimmerberg J. *J Membr Biol* 1995;(146):1-14.

EIS data. The changes in the EIS spectra upon tBLM completion attest for the formation of a complete tBLMs. In particular, the semicircular diameter in the Cole – Cole plot, proportional to the layer capacitance, shrunk from ~ 6 to $0.74 \mu\text{F}/\text{cm}^2$ (Fig. I.8, Table V), which is consistent with the formation of the phospholipid bilayer, as it was shown earlier (see Table I). Also, the membrane resistance (R_{def}) is increased, as expected for the formation of a well-sealed tethered lipid bilayer with the residual conductance, $Y_{tBLM} = 8 \cdot 10^{-6} \text{ S}/\text{cm}^2$. All this indicates that the vesicles of lipid extract have been successfully fused on the surface. These results demonstrate that by using vesicle fusion on a dense HC18 SAMs it is possible to transfer lipid extracts from natural objects to the surface creating artificial membrane models.

Table V. Best – fit parameters (model in Figure 1) to electrochemical impedance spectra of SAM and tBLMs from Fig.9 before and after vesicles fusion. The values of parameters are normalized to A_{el} .

<i>EIS</i> <i>parameters</i>	<i>SAM</i> (β -ME : HC18 = 3:7)	<i>After fusion with</i> <i>neuron membrane</i> <i>extract vesicles</i>
$CPE, \mu\text{F}/\text{cm}^2$	6.28	0.74
α_{tBLM}	0.9926	0.98
$R_{def}, k\Omega \cdot \text{cm}^2$	-	123.9
$Y_{tBLM}, \mu\text{S}/\text{cm}^2$	-	8.01

Chapter II. The investigation of pore forming toxins interaction with membranes

Pore – forming toxins, as the name suggests, disrupt the selective influx and efflux of ions across the plasma membrane by inserting a transmembrane pore. The tBLMs allow monitoring the incorporation and function of channel proteins by changes of their EIS response. In the current study, the PFTs: α -hemolysin (α -HL) from *S. aureus*²¹, anthrax toxin (PA₆₃) from *B. anthracis*²² and cholesterol dependent cytolysin vaginolysin (VLY) from *Gardnerella vaginalis*²³ were studied using tBLMs designed by us.

Reconstitution of α -hemolysin

The effect of reconstitution of α -HL into the phospholipid membrane is shown in Figure II.1 the toxin action is readily seen from the changes of EIS plots. In particular, upon incubation of tBLMs with α -HL, The Cole-Cole (Figure II.1) plot exhibits the complex capacitance increase, and most importantly, the appearance of the low

²¹ Song L, Hobaugh MR, Shustak C, Cheley S, Bayley H, Gouaux JE. *Science* 1996; (274): 1859-66.

²² Petosa, C.; Collier, R. J.; Klimpel, K. R.; Leppla, S. H.; Liddington, R. C. *Nature* 1997;(385): 833–838.

²³ Hotze E.M. and. Tweten R.K. *Biochimica et Biophysica Acta* 2012;(1818):1028-1038.

frequency tail. All these spectral features attest for the damage of the DPhPC membrane by the α -HL. This conclusion is supported by the changes of the Bode plots (Figure II.1 B), which after interaction with the PFT develops a step-like kink and the minimum on a $|Z|$ vs. frequency and $-\varphi$ vs. plots, respectively.

By fitting the equivalent circuit models (Figure 1 in Methods section) to the data from EIS spectra (Figure II.1 A and B) we obtained mean values for membrane capacitance and membrane conductance (Table VI). In this model, the capacitance is $C_{\text{BLM}} = 0.83 \mu\text{F}/\text{cm}^2$ for α -HL free membrane and $C_{\text{BLM}} = 1,05 \mu\text{F}/\text{cm}^2$ with α -HL. The value of capacitance is increasing $\sim 20\%$ in presence α -HL. The model derived conductance of membrane is $Y = 3.77 \mu\text{S}$ without α -HL and $Y = 54,01 \mu\text{S}$ when α -HL reconstitutes into tBLM. The index of parameter CPE_{def} is increasing from 0.56 to 0.82., and α_{def} is approaching 1. All these features are indicative of the rising defect density in tBLM.

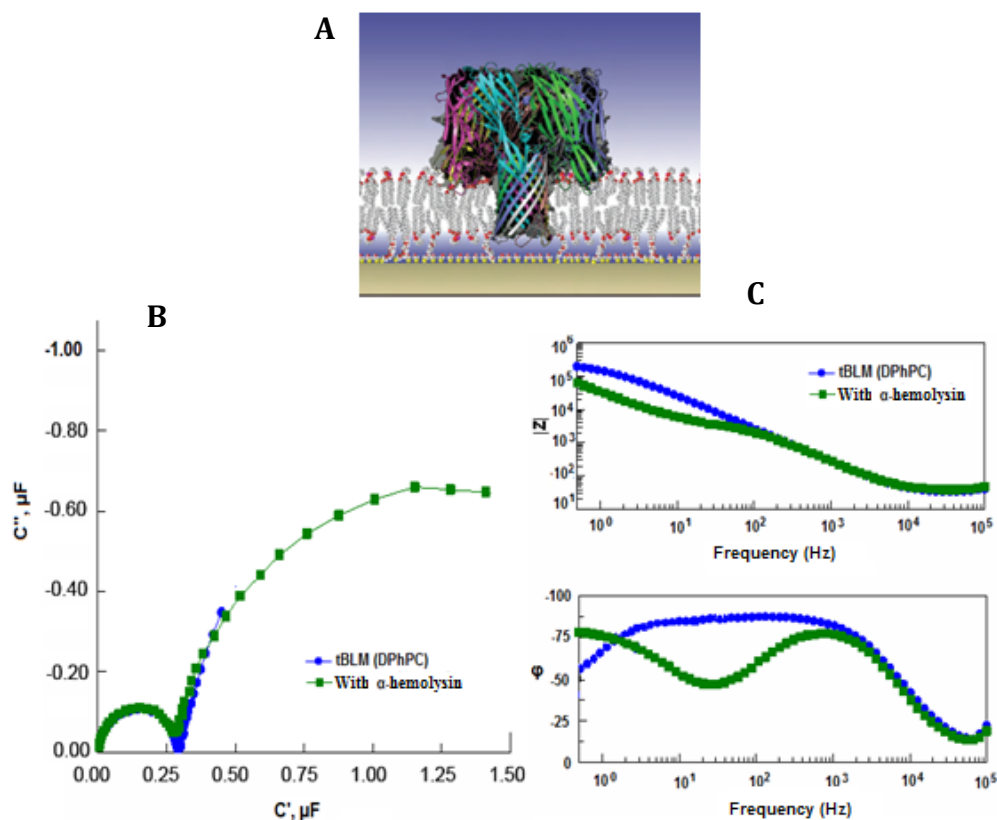


Figure II.1. Interaction between α -HL and DPhPC bilayer based on mixed SAM (WC14:ME = 3:7). **A.** Model of α -Hemolysin reconstitution into the artificial membrane²⁴. **B** - Cole cole plot of complex capacitance: blue – the initial spectra of tBLM, green – 50 min after α -HL of 140 nM injected. **C** – Bode plot of conducting tBLM: blue – the initial curve, green – 50 min after α -HL of 140 nM injected. In both figures is the same sample. An aqueous solution – NaCl 0.1M with 0.01 M phosphate buffer system at pH 7.4.

²⁴ McGillivray D.J., Valincius G., Heinrich F., Robertson J.W.F., Vanderah D.J., Febo-Ayala W., Ignatjev I., Losche M., Kasianowicz J.J. *Biophysical Journal* 2009;96(4):1547-53.

Table VI. EIS model fits for an DphPC bilayer based on mixed SAM (WC14:ME = 3:7) as prepared and after incubation with α -hemolysin. Parameters are the averages from n=25 measurements and normalized to surface area.

<i>Parameters</i>	<i>Before α-HL reconstitution</i>	<i>After α-HL reconstitution</i>
$CPE_{tBLM}, \mu F/cm^2$	0.83	1.00
α_{BLM}	0.9849	0.9791
$CPE_{def}, \mu F/cm^2$	6.18	9.97
α_{def}	0.56521	0.81906
$R_{def}, k\Omega \cdot cm^2$	202.88	10.19
Fit quality parameter, $\chi^2 * 10^4$	2.38	1.37

Concentration dependence of PFT-induced conductance of tBLMs: α -HL and PA₆₃

The variation of EIS in the course of the interaction between the tBLM and PFT occurs in a concentration dependent manner. For example, the position of phase minimum and the corresponding value of the impedance correlated with the concentration of the PFT in the bathing solution (Figure II.2). Recent mathematical analysis showed these features are determined by the density of the protein pores (membrane defects).²⁵ This suggests a straightforward way of estimating toxin activity by the EIS.

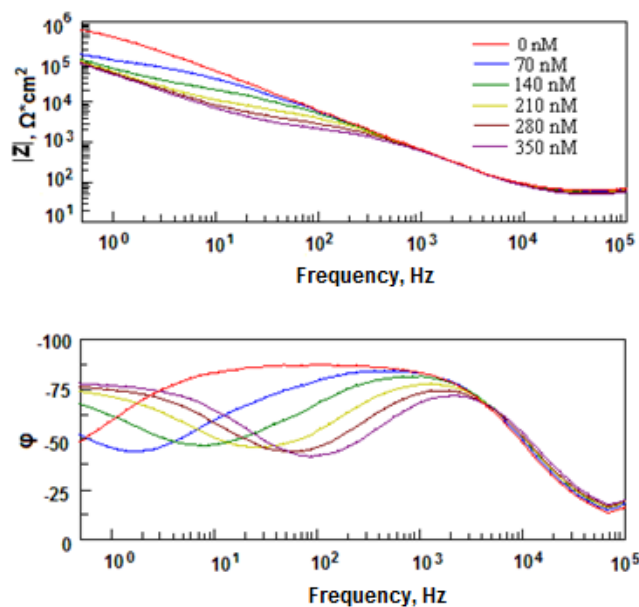


Figure II.2. The Modulus (A) and phase angle (B) of EIS spectra of an tBLM from DPhPC based on mixed SAM (WC14:ME = 3:7 in phosphate buffered NaCl (0.1 M), pH 7.4, as a function of α -HL concentration for no peptide (red line); 70 nM (blue); 140 nM of α -HL (green); 210 nM (yellow); 280 nM of α -HL (brown); 350 nM (purple). The spectra were measured 1h after the addition of α -HL to final concentration.

²⁵ Valincius G., Meskauskas T., and Ivanauskas F. *Langmuir*. 2012;(28):977-90.

To relate EIS features to a toxin concentration we have chosen a value of the conductance at the phase minimum on the Bode plots. We denote this values as a membrane conductance $Y_{tBLM} = (Z_{\text{phase min}})^{-1}$. Figure II.3. shows the variation of this parameter with a concentration of α HL and PA₆₃. It is obvious that Y_{tBLM} increases in a concentration dependent manner. Data in Fig. II.3 indicate that the Y_{tBLM} is not a linear function of PFT concentration, and it considerably depends on temperature. At the same time, it is obvious that the activity of PA₆₃ preparations were significantly higher. 10 nM concentration PA₆₃ triggered same response, which to achieve in case of an α HL would require tenfold concentration of α -HL.

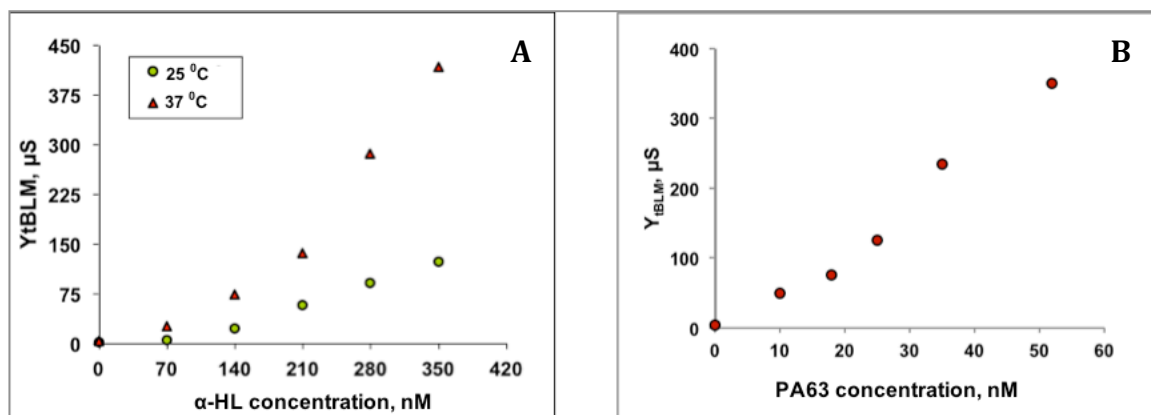


Figure II.3. **A.** The effect of α -HL on the conductance of BLMs as a function of α -HL concentration in range from 70 nM to 350 nM at 25 °C (green circles) and 37 °C (red triangles). **B** – Conductivity of DECoPC tBLMs as a function of PA₆₃ concentration (concentration range from 10 nM to 52 nM) in an aqueous solution – NaCl 0.1 M with 0.01 M phosphate buffer system at pH 7.4. Anchor SAM – WC:ME (30:70). The spectra were measured 1h after the addition of α -HL to final concentration.

Even though both toxins excreted similar EIS changes, their temporal response is different. The PA₆₃ injection, even at the concentration of 10 nM, resulted in a very rapid increase of conductance, which is in stark contrast to α -HL, which reconstitution required considerable time of incubation (60 min and more). This needs to be taken into account, when considering application EIS technique to assess activity of the PFTs.

Temperature dependence of PTF induced conductance of tBLMs

As it was demonstrated in Figure II.3A, the PFT-induced membrane conductance depends on the temperature. This dependency allows estimating the effective activation energy (E_a) of the ionic permeation through the toxin induced defects (pores).

The Arrhenius Y_{tBLMs} vs. T^{-1} plots for α -HL and PA₆₃ are shown in Figure IV. The plots are compared to those of the ion transport in the electrolyte used in the study.

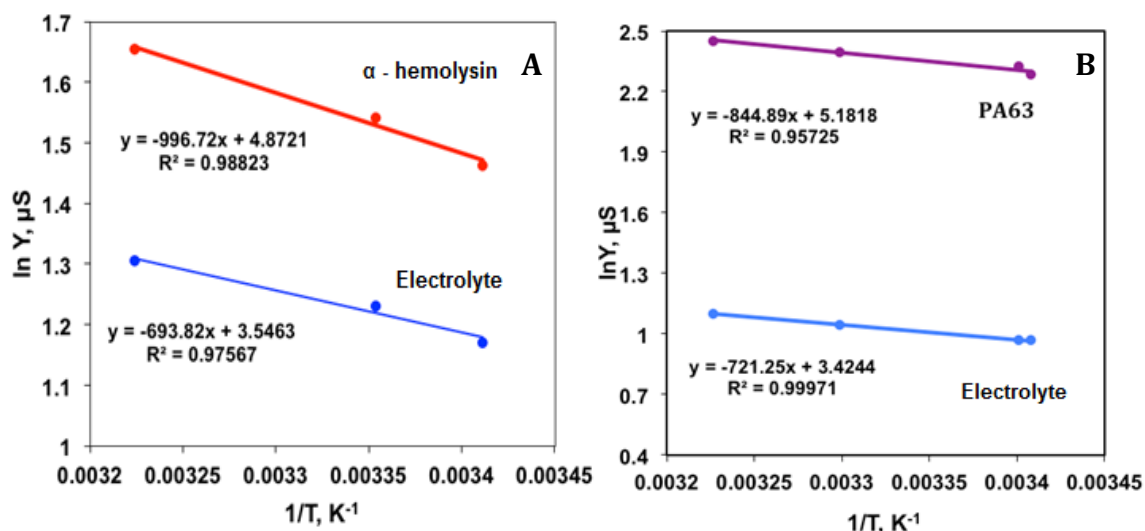


Figure II.4 A. Arrhenius plots of tBLM's conductivity $Y_{\alpha\text{HL}}$ vs T^{-1} (blue symbols), and solution electrolyte bulk conductivity vs T^{-1} (red symbols) measured in the same experiment. Measurements were carried out in sodium phosphate buffer on a DPhPC membrane. α -HL concentration is 140nM. Equations of the plot correspond to a best fit line of a data series, next to which an equation is located.

B – Arrhenius plots of tBLM's conductivity Y_{PA63} vs T^{-1} (purple symbols), and solution electrolyte bulk conductivity vs T^{-1} (blue symbols) measured in the same experiment. Measurements were carried out in sodium phosphate buffer on a DEcoPC membrane. PA63 concentration is 25 nM. Equations of the plot correspond to a best fit line of a data series, next to which an equation is located.

The activation barriers of ion transport, calculated from the Arrhenius plot slopes for the α -HL and PA₆₃ toxins were found to be 9.8 kJ/mol, and 7.1 kJ/mol, respectively. (Figure II.4 A, red line, Figure II.4 B, purple line). The bulk solution conductivity activation barrier E_a , as calculated from the Arrhenius plot slope, was found to be between 5.5 and 7 kJ/mol, (Figure II.4, light blue lines). It is obvious, that the activation energy for ion transport through both α -HL and PA63 is close to that for the ion transport through bulk of the electrolyte. These results suggest that both toxins form water filled pores, in which the ions driven by the electric field are travelling in an environment similar to one that is inside the bulk of the solution.

Functionality of channels of α -hemolysin and PA63

If the PFT channels are functional in tBLMs, the ability of neutral polymers to enter nanometer scale pores can be probed by the EIS. Su polymers as PEG enter into the channel, displaces ions and reduces their mobility in the pore. Different size PEGs have been used to estimate the size of biological ion channels, such as α -HL.²⁶

Schematic illustration, taken from the ref.²⁷, of the toxin pore in the presence of penetrating polymer chains is shown in Fig. II.5 A. PEG entry into the pore changes the

²⁶ Bezrukov, S. M.; Vodyanoy, I.; Brutyan, R. A.; Kasianowicz, J. J. *Macromolecules* 1996; (29): 8517.

²⁷ Bezrukov, S. M.; Vodyanoy, I.; Brutyan, R. A.; Kasianowicz, J. J. *Macromolecules* 1996; (29): 8517.

pore conductance thus signaling the polymers's presence, while the exclusion of the macromolecules from the pore triggers the osmotic stress that is followed by an increase of the conductance in the pore.

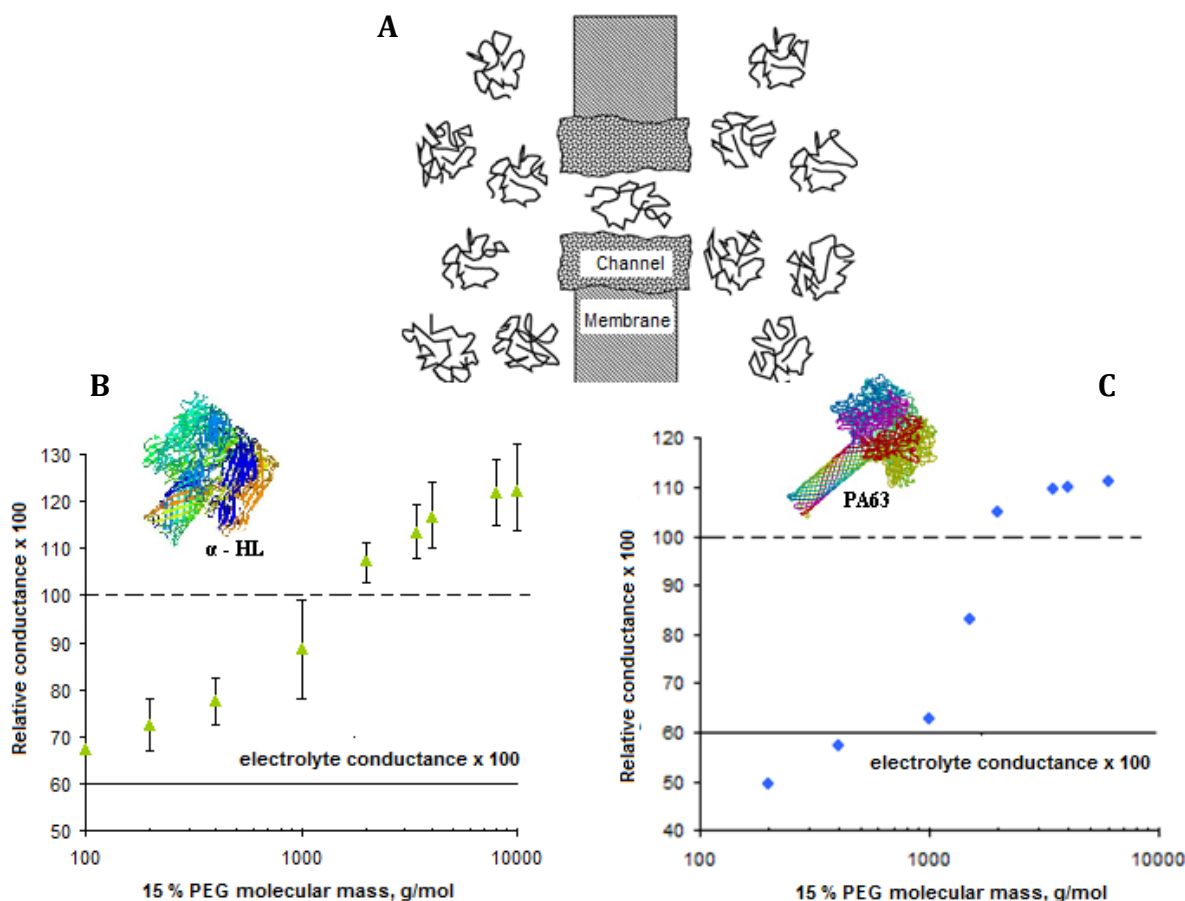


Figure II.5. The effects of different molecular weight PEGs on α -HL channel conductance. **A** – Schematic illustration of the toxin pore in the presence of penetrating polymer chains²⁸. **B** The PEG molecular weight (was used 15 % concentrations) dependence on conductivity of DPhPC tBLMs with α -HL (140 nM) in system. Anchoring SAM – Wcomp:ME (30:70). **C** – The PEG molecular weight (was used 15 % concentrations) dependence on conductivity of DEcoPC tBLMs based on with PA₆₃ (25 nM) in system.

Data in Figure II.5 B ir C shows that α -HL and PA₆₃ pores in tBLMs are blocked by the low molecular weight polymers, while the high weight PEGs are excluded. The effect of PEG on the α -HL channel of membrane conductance: PEGs with molecular weights ≤ 1000 partition into the pore and decrease the pore's conductance. Higher molecular weight PEGs, which do not partition into the pore, increase the conductance (Fig. II.5 B), because an osmotic effect²⁹ In case of PA₆₃ channel, the membrane conductance decreases in solutions containing PEGs with the molecular weights ≤ 2000 , while the higher molecular weight PEGs increase the conductance of pores (Fig. II.5

²⁸ Bezrukov, S. M.; Vodyanoy, I.; Brutyan, R. A.; Kasianowicz, J. J. *Macromolecules* 1996; (29): 8517.

²⁹ Joseph W. F. Robertson, Claudio G. Rodrigues, Vincent M. Stanford, Kenneth A. Rubinson, Oleg V. Krasilnikov and John J. Kasianowicz.. *PNAS* 2007; (104): 8027-42.

C). This suggests that the radius of the PA63 channel is comparable to radius of α HL pore.

Interaction of vaginolysin with tBLM

The cholesterol-dependent cytolysins (CDCs) constitute a large family of pore – forming toxins that function exclusively on a cholesterol containing membranes.³⁰ The CDC cytolytic mechanism requires the presence of the membrane cholesterol and the cholesterol has been considered to be the receptor for the CDCs. In this study we examined one of the member of this family, vaginolysin, VLY, in particular, its ability to reconstitute tBLMs.

VLY is a toxin that incorporates spontaneously into cholesterol containing membranes by the formation of large β -barrel pores. Its functional reconstitution into the bilayer should lead to a drastic decrease in the membrane resistance. So, it should be easily monitored by the EIS.

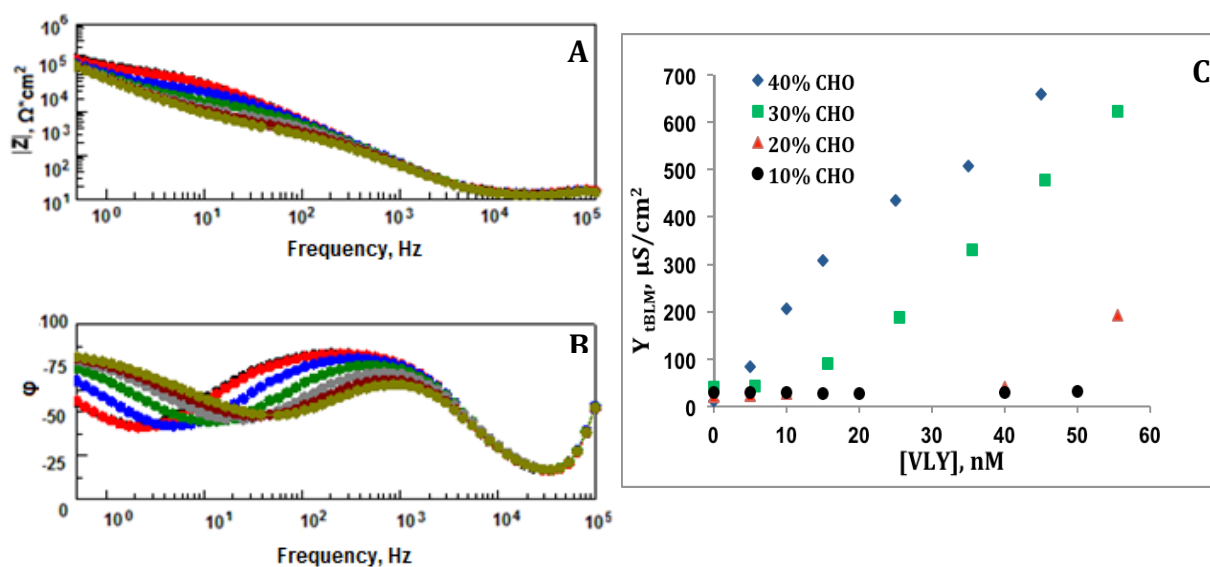


Figure II.6. The Modulus (A) and phase angle (B) of EIS spectra of an tBLM from DOPC/CHO 30% based on mixed SAM (HC18:ME = 3:7 in phosphate buffered NaCl (0.1 M), pH 7.4, as a function of VLY concentration: for no peptide (black); 5.8 nM (red); 15.6 nM of α -HL (blue); 25.6 nM (green); 35.6 nM of α -HL (grey); 45.6 nM (brown) and 55.6 nM (olive). The spectra were measured 30 min after the addition of VLY to final concentration.

Figure II.6 (C). Kinetics of VLY channel formation in tethered bilayer lipid membranes in variation of composition of bilayer. The concentration range of VLY is from 5.8 nM to 55.6 nM. tBLMs prepared on SAM (β -ME : HC18 = 7:3) and completed with DOPC with different amount of cholesterol: 10 % of cholesterol, CHO10% (black circles), 20 % of cholesterol (red triangles), 30 % of cholesterol (green squares) and 40 % of cholesterol (blue diamonds). The spectra were measured 30 min after the addition of VLY to final concentration.

The effect of VLY on tBLM EI spectra is shown in Fig. II.6. The Bode diagrams

³⁰ Heuck A.P., Tweten R.K. and Johnson A.E. *The JBC*. 2003;(278): 31218–25.

of DOPS/CHO30 tBLMs exhibit a clear concentration dependent response to the VLY toxin. Bode diagrams indicate, as expected, a decrease in the membrane resistance, Z at low frequencies, (Fig II.6 A) and continuous shift of the phase minimum with VLY concentration (Fig. II.6 B). A clear confirmation of VLY sensitivity to cholesterol stems from the data shown in Fig. II.6 C. The Y_{tBLM} increase rate accelerates with the amount of the cholesterol in the tBLM. Negative control tests on a cholesterol-free DOPC and OPPC tBLMs showed no effect on their EI spectra, confirming the cholesterol-dependent nature of the interaction between tBLMs and VLY. The spectral features, as in the case of α -HL and PA63 may be utilized for the bioanalytical detection of the toxin. So far, the lowest detectable level of VLY, in our experiments, was ~ 5.8 nM (Figure II.6 C).

Our study also indicates that at least in the model tBLM systems, the CD59, which is believed, is necessary for the anchoring and insertion of the toxin into the phospholipid membranes, was not required to observe membrane damage by VLY.

Chapter III. The study of interaction and neurotoxicity of $A\beta_{1-42}$ oligomers

Amyloid oligomers are believed to be implicated into the Alzheimer's pathogenesis. Many different laboratories have reported the effects of amyloid oligomers that were dependent on the size, morphology, toxicity, as well as the methods of preparation or purification. This raises the question of the relationship between these properties and possible toxicity of amyloid species implicated in neurodegeneration³¹.

The purpose of the present work is to establish and quantify the dependence of neurotoxic effects on the size and morphology of synthetic $A\beta_{1-42}$ oligomers.

1. The morphology and structure of $A\beta_{1-42}$ aggregates

The characterization of $A\beta_{1-42}$ oligomers and fibrils by the atomic force microscopy

This part of the work represents a study of the oligomerization conditions on the morphology of $A\beta_{1-42}$. The study was performed by AFM using $A\beta_{1-42}$ preparations precipitated on a freshly cleaved mica.

$A\beta_{1-42}$ assembly is dependent on incubation time. Incubation time is a factor strongly affecting the size and morphology of $A\beta_{1-42}$ oligomers. By AFM we tested the incubation times: 24 h, 48 h, 72 h (data not shown). After 24 h incubation at room temperature the oligomer size reached 3 – 5 nm, after 48 h bigger oligomers with sizes 6 – 10 nm were observed. After a 72 h incubation at room temperature, fibrils, or protofibrils started to appear in $A\beta_{1-42}$ solutions.

$A\beta_{1-42}$ Assembly is dependent on temperature. Solutions of 70 μM $A\beta_{1-42}$ were incubated at 4 °C and 37 °C typically yielded different size and morphology species of $A\beta_{1-42}$. At room and 4 °C temperatures, the solution produced homogeneous of 2 – 4 nm oligomers.

³¹ Glabe C.G. *J Biol Chem.* 2008;(283):29639–43.

At 37 °C, the solution contained an increased number of protofibrils.

A β ₁₋₄₂ oligomers morphology is dependent on concentration of solvent, HFIP. Fluorinated alcohols including HFIP and trifluoroethanol have been shown to break down β -sheet structure, disrupt hydrophobic forces in aggregated amyloid preparations, and promote α -helical secondary structure. The AFM results show in Figure III.1, that HFIP concentration in amyloid prepreparation during the oligomerization process has a critical influence on the size of oligomers: 5 % of HFIP resulted in oligomer size of 2 – 4 nm (Fig. III.1 **A**); (hereinafter we refer to a z-height measured in AFM as a size of oligomers); 3.5 % of HFIP yield oligomers size of 3 – 8 nm (Fig. III.1 **B**); 0 % of HFIP – resulted in the formation of various kinds of aggregates and fibrillar structures that vary in z-height from 5 to more than 25 nm (Fig. III.1 **C**).

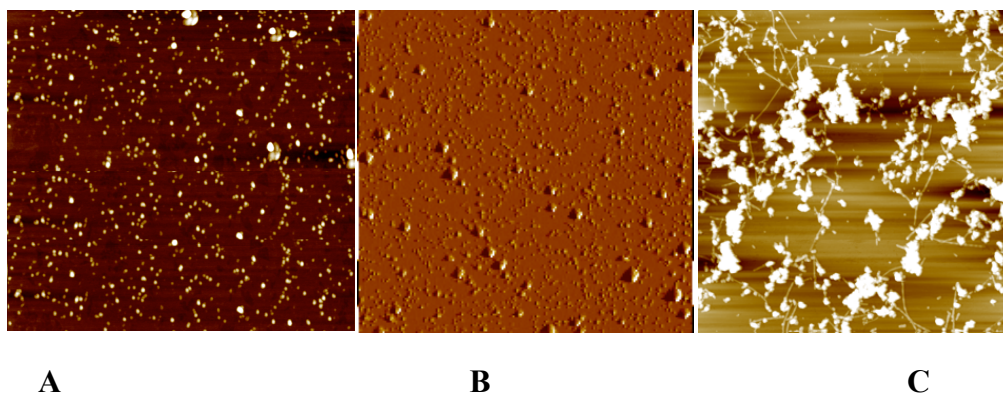


Figure III.1. A β ₁₋₄₂ assembly is dependent on HFIP concentration. **A.** HFIP amount in preparation: 5 % - time of evaporation 5min. **B** – HFIP 3.5 % - time of evaporation 7 min. **C** – HFIP 0 % - time of evaporation 30 min. Representative images in 8x8 μ m. In all cases the concentration of peptide was 10 μ M.

For the following analysis we will define three different types of amyloid species. Their morphologies are shown in Fig. III.2 **A** – **C**. they differ in both the morphology (oligomers vs. fibrils) and the size. AFM images in Figure III.2 **A-C** show that oligomers prepared by *protocol I* exhibited mean z-height values spanning from 1 to 3 nm (Fig. III.2 **A** and **D**), in few cases reaching 4 – 5 nm. In contrast, *protocol II* yielded considerably larger rounded species with size of 5 – 10 nm. . Finally, fibrillar, micrometer length structures were obtained by *protocol III*.

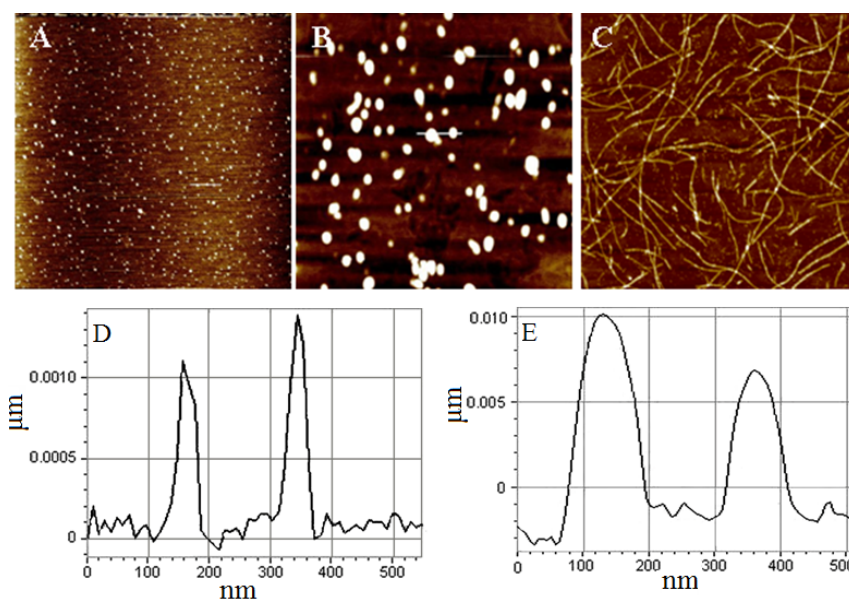


Figure III.2. Exemplary AFM images of $A\beta_{1-42}$ oligomers prepared by the different protocols: (A) *protocol I*, (B) *protocol II*, (C) *protocol III*. The lateral size of the images is $4 \times 4 \mu\text{m}$. The horizontal bars in A and B show the location at which height profiles of the images were analyzed (D and E) are the corresponding cross sections of the particles obtained via *protocols I* and *II*.

The size of $A\beta_{1-42}$ oligomers in solutions. Fluorescence correlation spectroscopy and dynamic light scattering

AFM images were obtained on dried samples. To investigate how drying of the sample affects the aggregate sizes we carried out DLS and FCS measurements in solutions containing different forms of $A\beta_{1-42}$ oligomers. Both methods confirm that *protocol I* typically generates particles with sizes from 1 to 4 nm. Representative particle size distributions obtained with DLS are shown in Fig. III.3 A. Preparations obtained via *protocols I* (light gray) and *II* (dark gray) differ significantly. In this particular data set, *protocol I* $A\beta_{1-42}$ oligomers show an average diameter of 2.7 nm, while the *protocol II* particles had average diameter of 8 nm (assuming spherical particle shape). This result is consistent with the AFM data and suggests that drying for AFM imaging does not significantly alter particle size. FCS data obtained with fluorescently labeled aggregates indicated similar particle size distributions, which, in case of *protocol I* preparations (Fig. III.3 B) exhibits two maxima: one with the mean diameter at 3.4 nm and another with smaller intensity at 8 nm.

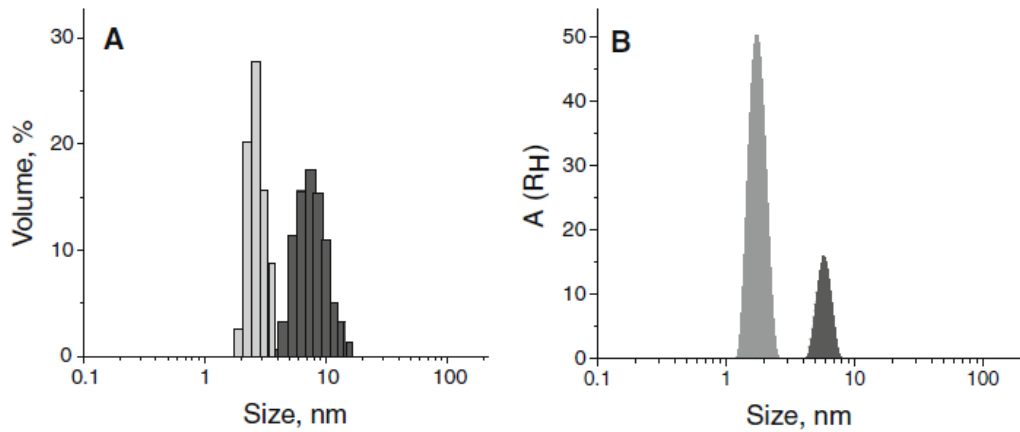


Figure III.3. Size distribution of differently prepared $A\beta_{1-42}$ oligomers. (A) DLS. Light gray: *protocol I* aggregates, dark gray: *protocol II* aggregates. The larger size oligomer preparation contained also a small contribution of sizes above 200 nm (not shown). (B) FCS results for *protocol I* and *II* oligomers with the same coding as in panel (A).

Size dependent neurotoxicity of $A\beta_{1-42}$ oligomers

The relationship between the toxicity of $A\beta_{1-42}$ oligomers and their size is presented in Fig. III.4 At $1\mu\text{M}$ concentration, small $A\beta_{1-42}$ particles (1 – 2 nm z-height in AFM) obtained by *protocol I* were highly toxic to neurons: after 24 h of incubation just 10 – 40 % of viable neurons were observed. Toxicity of $A\beta_{1-42}$ decreased with increase in the size of the particles: 50 – 85 % of viable cells were observed after incubation with medium sized $A\beta_{1-42}$ particles (3 – 5 nm z-height, *protocols I* and *II*). Larger particles (5 – 9 nm z-height, *protocol II*) were non-toxic to neurons.

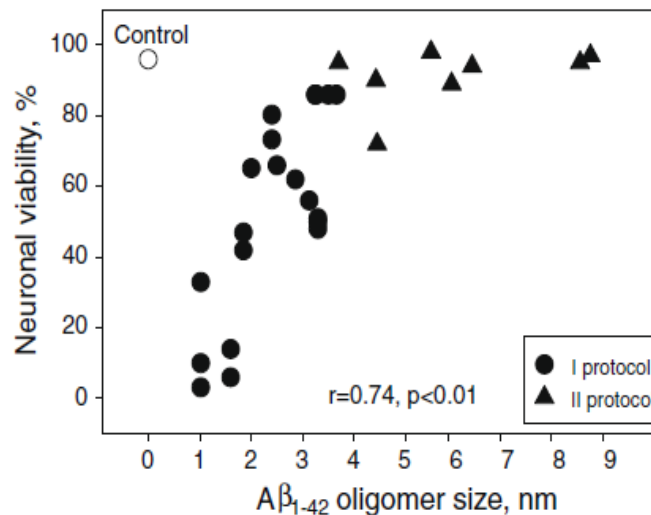


Figure III.4. Toxicity of $A\beta_{1-42}$ oligomers depends on aggregate size as determined with the AFM in terms of z-height. $A\beta_{1-42}$ oligomers were prepared by *protocols I* and *II*. CGCs were treated with 1IM $A\beta_{1-42}$ oligomers for 24 h. Each point represents the effect of a separate preparation of oligomers on viability of separate CGC culture (mean values are presented for each experiment).

This suggests that the neurotoxicity correlates with the $A\beta_{1-42}$ oligomer size (Pearson's correlation coefficient $r = 0.74$) rather than with the protocol, by which the particles are generated, as small oligomers prepared by *protocol I* are the main cytotoxic species but larger particles prepared by either *protocols I* and *II* show comparably low cytotoxicity. Notably, even though the cytotoxicity of $A\beta_{1-42}$ oligomers of different sizes differs significantly, neither the CD spectra nor the IR measurements indicate differences in their secondary structure. This points out to the size of oligomers as a primary factor responsible for the cytotoxicity observed in the current work.

Toxic and non-toxic $A\beta_{1-42}$ aggregates interact differently with phospholipid membranes

To assess whether different size oligomer preparations bind differently to phospholipid membranes we carried out vesicle binding test using FCS. Fig. III.5 shows FCS correlation curves fitted with appropriate 3D diffusion models for two different size oligomers preparations. The experiment sequence was as follows. First, was recorded autocorrelation of oligomers prepared via *protocols I* (Fig. III.5 A) and *II* (Fig. III.5 B) diffusing freely in solutions without vesicles (red dots). These data were fitted with a single component 3D diffusion model shown as red continuous lines, and provides diffusion times of 0.05 and 0.20 ms for small and big oligomer preparations, respectively. Second, both oligomer batches were brought into contact with lipid vesicles, and changes of the autocorrelation curves were recorded (black dots).

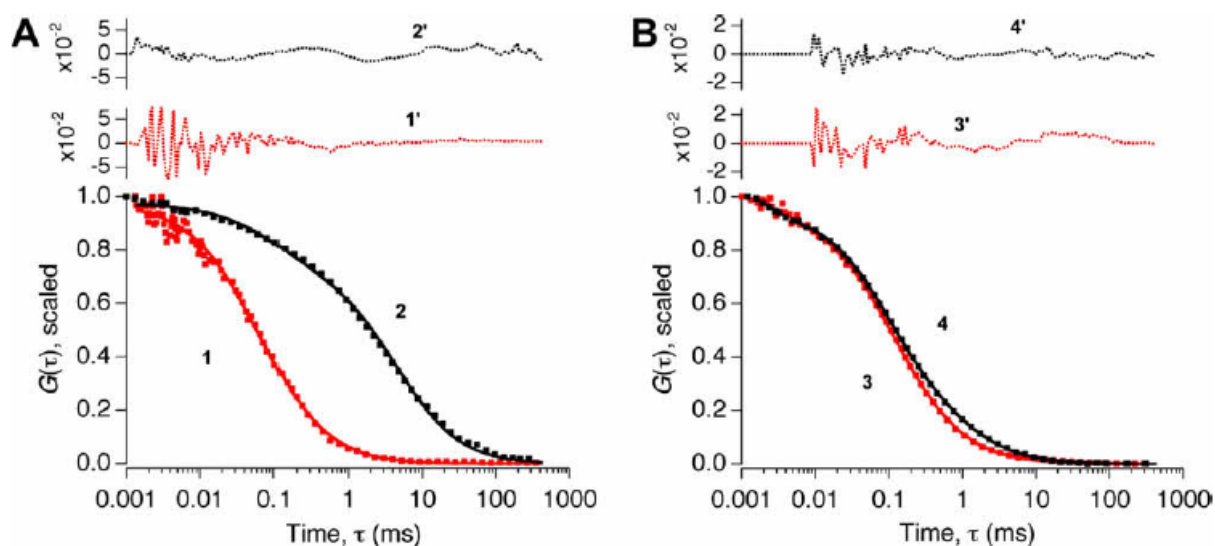


Figure III.5. Different size $A\beta_{1-42}$ oligomers bind differently to lipid membranes. FCS data (dots) are fitted (continuous lines) with a single component 3D diffusion model for fluorescently labeled $A\beta_{1-42}$ diffusing freely in bulk (red curves 1 – 3) and with a two – component 3D diffusion model for $A\beta_{1-42}$ diffusing in the presence of nonfluorescent lipid vesicles (black curves 2 and 4). Residuals of the fits are shown at the top of each panel (curves 1 – 4). (A) Small $A\beta_{1-42}$ oligomers (*protocol I*), (B) big oligomers (*protocol II*).

The FCS data in Fig. III.5 **A** and **B** show that different size $A\beta_{1-42}$ oligomers bind differently to the phospholipid membrane. While the small oligomers prepared via *protocol I* causes a significant shift of the FCS curve towards longer correlation times, the big ones prepared via *protocol II* exhibit just a marginal effect. The increase of the correlation time indicates a slowdown of the thermal motion of the fluorescently labeled particles, which may occur only if the $A\beta_{1-42}$ particles bind vesicles. This result indicate a clear difference in binding propensity of the different size oligomers. Small, and toxic oligomers exhibit higher affinity towards the phospholipid bilayers.

Toxic $A\beta_{1-42}$ oligomers species affect dielectric properties of tBLMs

Accumulation of the amyloid protein ($A\beta_{1-42}$) in the brain is an important step in the pathogenesis of Alzheimer's disease. However, the mechanism by which $A\beta_{1-42}$ exerts its neurotoxic effect is largely unknown. Data in the previous section suggests strong interaction of $A\beta_{1-42}$ preparations with phospholipid membranes. This interaction may alter the insulating properties of the phospholipid membranes through two mechanisms: ion channel formation and the decrease of the dielectric barrier³².

Fig. III.6 **A**, shows the effect of incubation of tBLMs with soluble $A\beta_{1-42}$ oligomers. The presence of $A\beta_{1-42}$ oligomers leads to a characteristic reduction of the membrane impedance, Z , in the low frequency range.

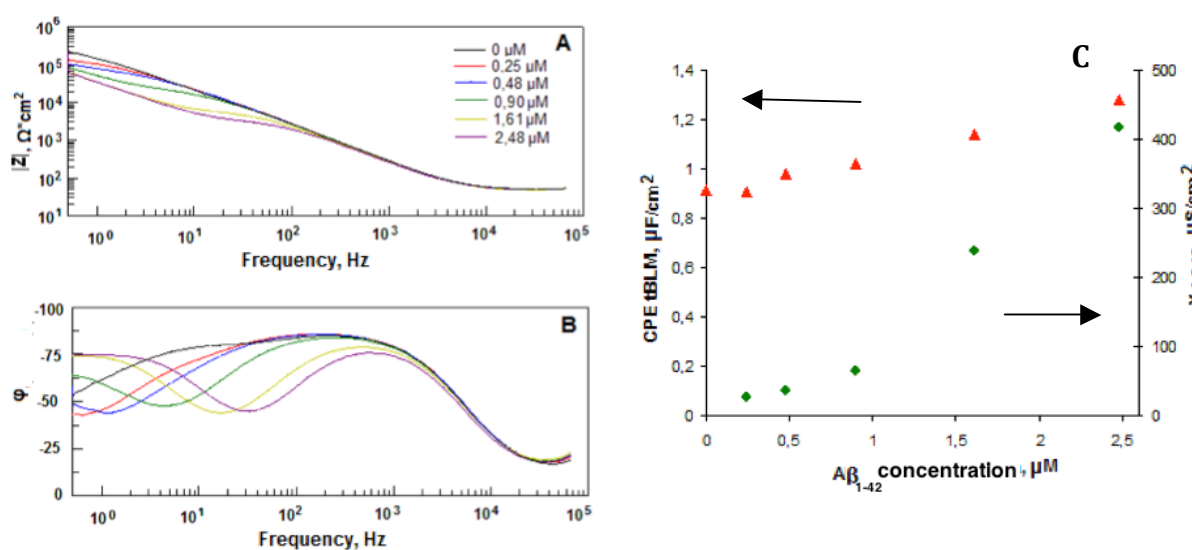


Figure III.6. Modulus (**A**) and phase angle (**B**) of electrochemical impedance spectra of an tBLM (WC14:bME = 3:7 + DOPC) in phosphate buffered NaCl (0.1 M), pH 7.4, as a function of $A\beta_{1-42}$ oligomers concentration for no peptide (black); 0.25 μM (red); 0.48 μM (blue); 0.90 μM (green); 1.61 μM (yellow); 2.48 μM (purple). (**C**) Impact of soluble prefibrillar $A\beta_{1-42}$ - oligomers on membrane capacitance and conductance in an tBLM (as a function of peptide concentration, measured on one single bilayer. The impact on tBLM capacitance (triangles) and tBLM conductance (diamonds) is shown.; triangles and diamonds are best-fit parameters from a model that describes data sets such as those shown in the main panel A and B.

³² Kaye R. Head, E., Thomson J.L., McIntire T.M., Milton, S.C., Cotman, C.W., Glabe, C.G. *Science*. 2003, 300, 486–9.

In addition, the phase minimum appears, and it moves towards higher frequencies as the concentration of A β ₁₋₄₂ amyloids increases (Figure III.6 B). Similar spectral signatures, as have been showed in Chapter II, are typical for the response of tBLMs at incubation with the pore-forming toxins (Figure II.2 and II.6).

The conductance $Y_{A\beta_{1-42}}$, which is the A β ₁₋₄₂ oligomer induced conductance at the phase minimum (estimated as $Y_{A\beta_{1-42}} = Z_{\text{phase min}}^{-1}$), and the tBLM capacitance, CPE_{tBLM} , are plotted in Fig. III.6 C as a function of the peptide concentration. Fig. III.6 C shows that $Y_{A\beta_{1-42}}$ depends on peptide concentration in a nonlinear manner, while the capacitance is almost linear. Data in Figure III.6 C indicate that A β ₁₋₄₂ affects both the capacitance, and membrane conductance simultaneously. This suggests that the dielectric damage that alters the ion movement through the membrane barrier may be responsible for the leakage of tBLMs affected A β ₁₋₄₂ oligomer.

Activation energies of ion transfer across membranes affected by the A β ₁₋₄₂ oligomers

Activation energy of the A β ₁₋₄₂ oligomer induced membrane conductance was determined using the dependence of $Y_{A\beta_{1-42}}$ vs. T^{-1} . This plot was compared to the one of the ions in the bulk of the electrolyte, and ion translocation through an α -HL pore (Figure III.7). The slopes of the Arrhenius plots yield the activation energy (E_a) for the A β ₁₋₄₂ oligomer induced conductance of $E_a = 37$ kJ/mol for a DOPC tBLM. These values are much higher than the activation energies for the ion conductance in the bulk electrolyte, $E_a \approx 6$ kJ/mol. It is also much higher than the activation barrier or an α -HL induced conductance, $E_a \approx 10$ kJ/mol.

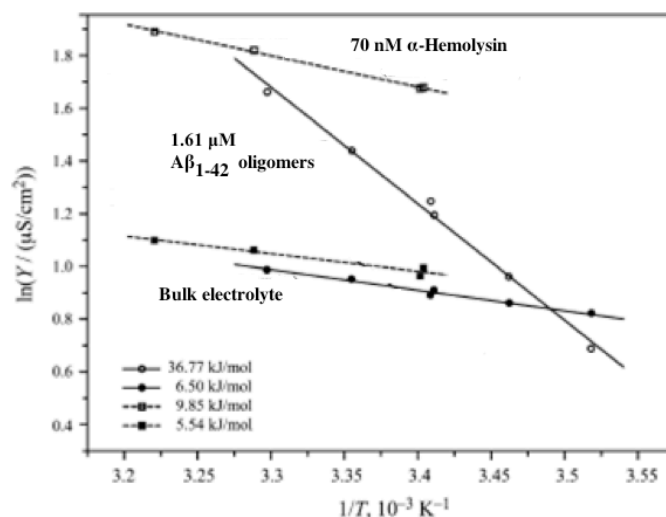


Figure III.7. Arrhenius plots of ion conductance across bilayers induced by soluble A β ₁₋₄₂ oligomers or by α -Hemolysin, and in the electrolytes bathing these bilayers. In tBLMs, the conductance was derived from modeling EIS data with the equivalent model (Fig. 1). Therefore, bulk electrolyte conductance (solid squares and circles) and membrane conductance (open squares and circles) were determined in the same experiment. The tBLM, was composed of WC14:bME (3:7) and DOPC; for incubation with A β ₁₋₄₂ (circles) and with DPhPC for tBLM reconstituted with α -HL (squares) In contrast, α -HL was studied in DPhPC-based tBLMs, because these kind of membranes are used for α -HL reconstitution³³.

³³ McGillivray D.J., Valincius G., Heinrich F., Robertson J.W.F., Vanderah D.J., Febo-Ayala W., Ignatjev I., Losche M., Kasianowicz J.J. *Biophysical Journal* 2009;96(4):1547-53.

In contrast to α -HL, the barrier of the $A\beta_{1-42}$ oligomer induced conductance depends pronouncedly on peptide concentration. Large conductance activation barrier for ion movement through the $A\beta_{1-42}$ oligomers perturbed its dependence on peptide concentration suggests different ion permeation mechanism than the one observed in the PFT cases. It is likely that the $A\beta_{1-42}$ oligomers produces water devoid narrow pathways in the membrane or the ion transfer might occur directly through the thinned dielectric phospholipid layer or $A\beta_{1-42}$ oligomer produced higher dielectric constant domains (see capacitance increase in Fig. III.6 via the solubility-diffusion mechanism).

The membrane affinity of $A\beta_{1-42}$ oligomers prepared by the “NaOH protocol”

To test how the absence of the fluorinated anti-oligomerization agents affects $A\beta_{1-42}$ oligomers properties and their interaction with tBLMs, we used the so-called *NaOH protocol* (see Methods section of the Dissertation) which avoids the usage of HFIP.

NaOH protocol produced $A\beta_{1-42}$ oligomers of significantly larger size, which caused the EIS spectral changes (Fig. III.8) qualitatively similar to those observed for $A\beta_{1-42}$ oligomers prepared using HFIP. In particular: a) a V-shaped part of the curve in the Cole-Cole spectra (Fig. III.8 A), “lifts off” the x-axis and moves “northwest” in the complex plane.

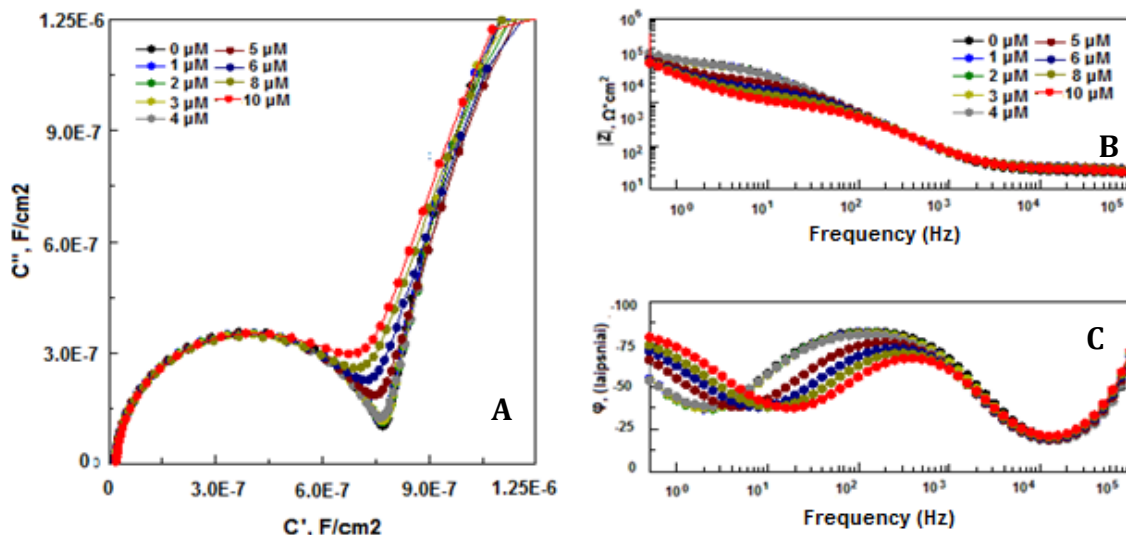


Figure III.8. Impact of soluble $A\beta_{1-42}$ oligomers produced by the produced by the *NaOH protocol* on **A)** the complex capacitance (Cole-Cole plots), **B)** impedance magnitude vs. frequency (Bode) plots and **C)** impedance phase vs. frequency (Bode) plots. tBLMs are accomplished on mixed SAMs (HC18:bME (3:7)) and completed with the DOPC/CHO/SM phospholipid mixture. $A\beta_{1-42}$ oligomer concentrations are: black – 0 μ M, blue – 1 μ M, green - 2 μ M, yellow – 3 μ M, grey - 4 μ M, brown - 5 μ M, purple – 6 μ M, olive – 8 μ M, red - 10 μ M. The spectra were measured immediately after the addition of $A\beta_{1-42}$ to the solution.

From the recent mathematical analysis such change in the Cole-Cole EIS plots signals the increase in the membrane defect density³⁴; b) on the Bode plots Z vs. frequency a plateau appears, which shifts down with the $A\beta_{1-42}$ concentration signaling an increase of the conductance of tBLMs (Fig. III.8 B); c) Third, on phase vs frequency plots a minima develops, which shift towards high frequency edge of the spectra with $A\beta_{1-42}$ concentration (Fig. III.8 C) retaining the impedance phase value unchanged. According to the theory,³⁵ such features are observed when the membrane defects are distributed evenly across the tBLM. Such feature does not occur, in case of defect clustering.

Membrane composition was found to be one of the important factors affecting the ability of *NaOH protocol* $A\beta_{1-42}$ oligomers to bind and affect properties of tBLMs. For this purpose, we compared tBLMs prepared using different phospholipid mixtures: pure DOPC, DOPC/DOPS10%, DOPC/CHO30% and DOPC/CHO30%/SM7% (molar percentage is indicated).

Figure III.9 shows plots of $A\beta_{1-42}$ oligomer induced conductance as a function of peptide concentration. The conductance remains almost unchanged up to a concentration of 4 μM concentration (Figure III.9) in all tBLMs. Beyond that concentration point the conductance starts increasing indicating damage to tBLMs by the oligomers. The most pronounced effect was observed on membranes containing sphingomyelin. Such sensitizing property of the sphingomyelin might be useful in practical applications where the sensitivity of the tBLMs system is crucial for the detection of minute amounts of membrane damaging $A\beta_{1-42}$ species.

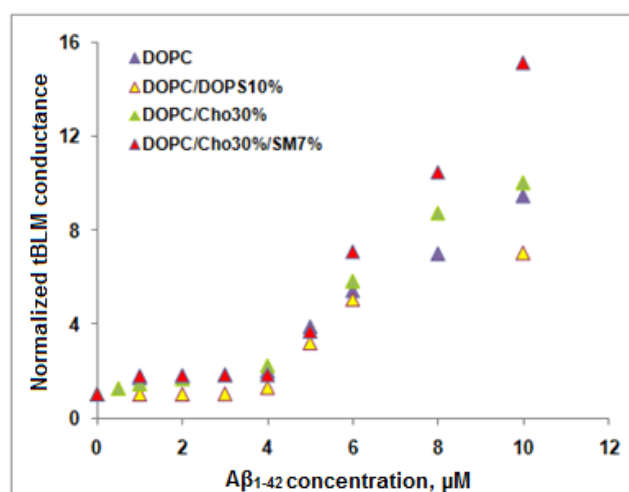


Figure III.9. Kinetics of VLY channel formation in tethered bilayer lipid membranes in variation of composition of bilayer. The concentration range of $A\beta_{1-42}$ oligomers is from 0 μM to 10 μM . tBLMs prepared on SAM ($\beta\text{-ME} : \text{HC18} = 7:3$) and completed with DOPC with different composition of bilayer, were: only DOPC (purple); DOPC/DOPS, were DOPS 10% (yellow), DOPC/CHO30%, were 30 % of cholesterol (green) and DOPC/CHO30%/SM7% of cholesterol (red).

³⁴ Valincius G., Meskauskas T., and Ivanauskas F. *Langmuir*. 2012;(28):977-90.

³⁵ Valincius G., Meskauskas T., and Ivanauskas F. *Langmuir*. 2012;(28):977-90.

Because the membrane damaging effect of *NaOH protocol* oligomers is obviously less pronounced than that of oligomers prepared using fluorinated compounds, we compared the activation barrier of the amyloid-induced conductance of tBLMs. Temperature effects on tBLM conductance were determined at the following concentrations: 3 μM for $\text{A}\beta_{1-42}$ oligomers prepared by *Protocol I*; at 5 μM for $\text{A}\beta_{1-42}$ oligomers prepared by mixed *NaOH/HFIP protocol*; at 10 μM for $\text{A}\beta_{1-42}$ oligomers prepared by *NaOH protocol*. Results are summarized in Fig. III.10.

Data in Figure III.10 clearly indicate that ion transport through the tBLMs exposed to *protocol I* (red triangles) $\text{A}\beta_{1-42}$ oligomers is higher than exposed to $\text{A}\beta_{1-42}$ oligomers prepared by the *NaOH protocol* (blue diamonds). The ion conductance barrier through the membrane exhibits activation energy of 11.6 kJ/mol in the case of *NaOH protocol* oligomers; 17.2 kJ/mol of $\text{A}\beta_{1-42}$ oligomers by *protocol I*; and 13.4 kJ/mol $\text{A}\beta_{1-42}$ oligomers formed using the mixed *HFIP/NaOH protocol*. The activation energy of the conductance in the bulk of the solution, in all cases, was 5.5 kJ/mol.

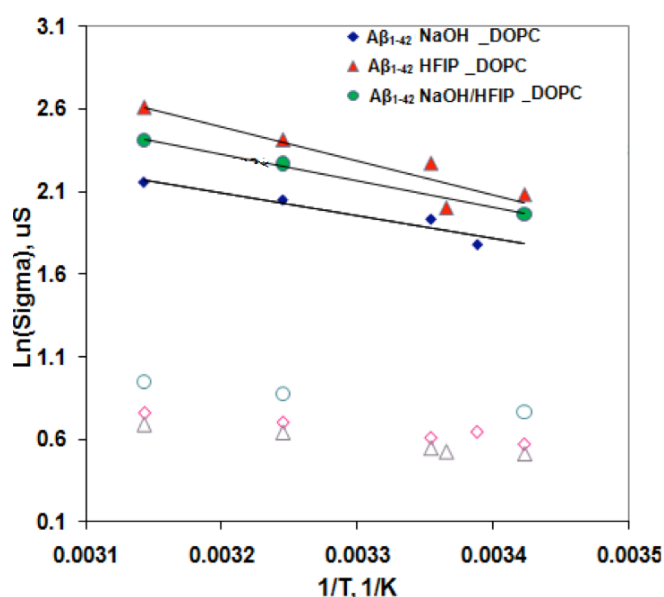


Figure III.10. Arrhenius plots of tBLM's conductivity $Y_{\text{Ab1-42}}$ vs T^{-1} (filled symbols), and solution electrolyte bulk conductivity vs T^{-1} (empty symbols) measured in the same experiment. Calculated E_a values are respectively for membrane affected by differently prepared $\text{A}\beta_{1-42}$ oligomers: $\text{A}\beta_{1-42}$ oligomers prepared by *protocol I*, using HFIP (red triangles); $\text{A}\beta_{1-42}$ oligomers prepared using *NaOH protocol* (blue diamonds); and mixed *NaOH/HFIP protocol*, using both solvents (green squares) and electrolyte bulk conductivity processes (empty symbols). Measurements were carried out in sodium phosphate buffer on the DOPC membrane. Equations of the plot correspond to a best fit line of a data series, next to which an equation is located.

This data show several important points. First, the damage inflicted on the membrane is dependent of the protocol or preparation of amyloids. Second, the difference may be not only quantitative but also qualitative. Low activation barrier observed for *NaOH protocol* oligomers suggest fundamentally different ion translocation through a membrane mechanisms. While the activation energies above 20 kJ/mol makes ion movement through the channels mechanism highly unlikely, energies close to 10 kJ/mol may signal the formation of such channels. And third, some components of

biological membranes, such as sphingomyelin, may significantly alter the susceptibility of the membranes to an action of $A\beta_{1-42}$ oligomers. The sphingomyelin not only sensitizes the tBLM response to *NaOH protocol* $A\beta_{1-42}$ oligomers, but it also significantly lowers the barrier for the conductance induced by the *protocol I* $A\beta_{1-42}$ species. This property of the sphingomyelin will undoubtedly attract more attention both in the light of the fundamental understanding of possible damage of amyloid oligomers on biological membranes as well as the practical applications of tBLMs systems as a biosensor platform.

CONCLUSIONS

1. Were observed that molecular anchors (WC14, FC16, HC18) differently affects the electrical properties of tBLM and the lateral mobility of phospholipids. The high density membranes.
2. Was obtained, that the defectiveness of tBLMs are increasing of the immobilized phospholipids in the sequence: DPhPC < DOPC < DEcoPC < POPC < OPPC.
3. Was proved, that the lipid membrane extracts from cells can be immobilized onto the surface as functional tBLMs by the vesicle fusion with high resistance of tBLM.
4. The composition of tBLMs accomplished via rapid solvent exchange can be modified by the direct transport of lipid between vesicles and membrane.
5. Were determined that the insertion of cholesterol are transferred simultaneously into tBLMs by decreasing the electric capacitance and activating the cholesterol dependent cytolysins.
6. By EIS were observed, that Pore forming toxins inserts into tBLM in a concentration-dependent manner, form water electrolyte-filled pores, in which an activation barrier of ionic mobility is close to that in the bulk solution.
7. The interaction between VLY and tBLM were detected by EIS. The lowest detectable level of VLY, in our experiments was ~ 5.8 nM. Were proved, that cholesterol is essential for VLY functionality.
8. Three different forms of $A\beta_{1-42}$ aggregates were prepared *in vitro*. Strong correlation between the size of Ab_{1-42} oligomers and their toxicity to neuronal cells was observed. The most toxic Ab_{1-42} oligomeric particles were with the z-heights from 1 to 4 nm.
9. The higher affinity of small toxic Ab_{1-42} oligomers to the phospholipid bilayers compared to the non-toxic were observed, but the secondary structures estimated by circular dichroism and IR spectroscopies indicate no difference.
10. $A\beta_{1-42}$ oligomers alter the dielectric constant of the lipid bilayer in such a way as to facilitate charge translocation by a variety of conductance mechanisms.
11. Was determined, that sphingomyelin enhances membrane damaging effect of $A\beta_{1-42}$ oligomers in tBLMs by decreasing an activation barrier of amyloid-induced membrane conductance.

ACKNOWLEDGMENTS

Work on this thesis would not have been possible without encouragement and support from many people. First and foremost I offer my sincerest gratitude to my Ph.D. advisor, **dr. Gintaras Valinčius**, who has supported me during my thesis with his patience, enthusiasm, guidance and knowledge. He opened the window to the world of Membranes for me. Under his intellectual guidance, I found the passion of doing academic research and the courage of facing the ups and downs in the process. I have enjoyed every moment of the insightful discussion with him.

I would also like to express my thanks to my consultant **habil. dr. Gediminas Niaura** for helping with SFG measurements and for sharing his knowledge in the field of spectroscopy during the progress of my research work.

The work in this thesis has been part of a much larger project and I would like to thank all the people who have contributed. In particular I would like to thank: **dr. Vilmantė Borutaitė**, **dr. Ramunė Morkunienė** and **Paulius Čižas** from Lithuanian University of Health Sciences for the fruitful collaboration and for stimulating discussions; **dr. Aurelija Žvirblienė** from the Institute of Biotechnology Vilnius University for donating a Vaginolysin and making an A β ₁₋₄₂ antibodies; **dr. Justas Barauskas** for advising on AFM imaging; To company “Ekspla”, for allowing me to do experiments with SFG and for providing me with the necessary instrumentation.

I am very grateful to **dr. David Vanderah** (NIST, USA) for his kind gift of anchors molecules. Without his support, this work would not have been possible.

I would like to thank to **prof. Mathias Losche** (CMU and NIST, USA) for possibility to visit the Carnegie Mellon University (Pittsburgh, PA, USA) and be a part of your group, also for confidence. Specifically I thank you: **Sidd Shenoy** for teaching me to use a FCS and for friendly discussions; **dr. Radu Moldovan** for showing me a Pittsburgh and having fun after work; **Agnieszka Kalinowski** for welcoming me as a friend and helping with accommodation where I have felt like at home.

Thank you to **Dr. John J. Kasianowicz** (NIST, USA) for donating an antrax toxin.

I am grateful to **Mindaugas Mickevičius**, **Marija Jankunec** and **Tadas Ragaliauskas** for providing nice coffee breaks, sharing frustration and happiness and making life more interesting; and to all the past and present members of the Laboratory of Bioelectrochemistry and Biospectroscopy, for providing a pleasant and supportive working atmosphere.

Finally, I wish to thank my family; and to **Donatas (Džiugas)** for the love, support and never-ending patience.

LIST OF PUBLICATIONS

Articles

1. Valincius G., Heinrich F., **Budvytyte R.**, Vanderah DJ, Sokolov Y, Hall JE and Lösche M. Soluble amyloid β oligomers affect dielectric membrane properties by bilayer insertion and domain formation: Implications for cell toxicity. *Biophysical Journal*. 2008;95:4845-61
2. Paulius Cizas*, **Rima Budvytyte***, Ramune Morkuniene, Radu Moldovan, Matteo Broccio, Mathias Loesche, Gediminas Niaura, Gintaras Valincius, Vilmante Borutaite. Size-dependent neurotoxicity of b-amyloid oligomers. *Archives of Biochemistry and Biophysics*. 2010;496(2):84-92.
* These authors contributed equally.
3. G. Niaura, **R. Budvytyte**, Z. Kuprionis, G. Valincius. Sum frequency generation spectroscopy of amyloid fibrils and oligomers at air/water interface. *Proc. SPIE*, 2010;(7376):1-7.

Manuscripts in preparation

1. **Rima Budvytyte**, Mindaugas Mickevicius, David J. Vanderah, Frank Heinrich, Gintaras Valincius. Modification of tethered bilayer compositions by material exchange with vesicles. *Langmuir* 2012.
2. **Rima Budvytyte**, Gintaras Valincius, Gediminas Niaura, Vlada Voiciuk, Mindaugas Mickevicius, Hilary Stauffer Prabhanshu Shekhar, Frank Heinrich, Siddharth Shenoy, David J. Vanderah and Mathias Lösche. Anchor Molecules Affect Structure and Properties of Tethered Bilayer Lipid Membranes. *Prepared for the submission*. 2012.

Papers not included into the dissertation:

1. Vladislava Voiciuk, Gintaras Valincius, **Rima Budvytyte**, Algirdas Matijoska, Gediminas Niaura. Surface-enhanced Raman spectroscopy for detection of toxic amyloid β oligomers adsorbed on self-assembled monolayers. *Spectrochimica Acta Part A: Molecular and Biomolecular Spectroscopy*. 2012;(95): 526-532.

Handouts:

Matteo Broccio, Rima Budvytyte, Gintaras Valincius and Mathias Loesche. Tethered lipid bilayers that mimic neuronal membranes. *Biophysical Journal*, 2010;(98)3:271a-271a. 2010 02 20-24 Biophysical Society 54th Annual meeting. San Fransiskas, USA.

David J Vanderah, Gintaras Valincius, Rima Budvytyte, Gediminas Niaura, Vlada Voiciuk, Hilary Stauffer, Frank Heinrich, Prabhanshu Shekhar. Characterization of Tethered Bilayer Lipid Membranes. 2010 04 10-13 ACS Mid Atlantic Regional Meeting. Wilmington, Delaware.

G. Niaura, R. Budvytytė, G. Valincius, Z. Kuprionis. Sum frequency generation spectroscopy of amyloid fibrils and oligomers at air/water interface. 2010 06 9-11 XII International conference on Laser Applications in Life Sciences 2010 (LALS-2010), Oulu, Finland.

Rima Budvytyte*, Paulius Cizas*, Ramune Morkuniene, Radu Moldovan, Matteo Broccio, Mathias Loesche, Gediminas Niaura, Gintaras Valincius, Vilmante Borutaite. Size-dependent neurotoxicity of β -amyloid oligomers. *Both authors contributed equally. 2010 06 15-17 XI Tarptautinė Lietuvos Biochemikų draugijos konferencija, Tolieja, Lithuania.

Rima Budvytyte, Paulius Cizas, Ramune Morkuniene, Sidd Shenoy, Vilmante Borutaite, Mathias Lösche, Gintaras Valincius. Membrane Affinity and Neurotoxicity of b-amyloid Oligomers. *Biophysical Journal*, 2011;(100)3:511a. 2011 03 05-09 Biophysical Society 55th Annual Meeting, Baltimore, Maryland, USA.

Rima Budvytyte, David J. Vanderah, Gintaras Valincius. Formation and modification of Tethered Lipid Bilayer membrane (tBLM) by Vesicle Fusion. 2011 09 07-10 1st Central and Eastern European Conference on Thermal Analysis and Calorimetry (CEEC-TAC1). Craiova, Romania.

Rima Budvytyte, Tadas Ragaliauskas, Gintaras Valincius. "Multicomponent tethered bilayers by lipid exchanges with vesicles. 2012 07 23 -27. ICNT, International Conference on Nanoscience +Technology, Paris, France.

DIRBTINĖS FOSFOLIPIDINĖS SISTEMOS BALTYMŲ BEI PEPTIDŲ SĄVEIKOS SU BIOLOGINĖMIS MEMBRANOMIS TYRIMAMS

REZIUMĖ

Pagrindinis disertacijos objektas yra imobilizuotos fosfolipidinės membranos (tBLM) ant aukso paviršiaus, kurios pastaruoju metu panaudojamos kaip lipidiniai membranų modeliai tiriant baltymų įsiterpimą ir jų funkciją. Mes sukonstravome stabilias ir universalias tBLM, panaudodami tiolipidinius junginius (inkarus), kurie šiose sistemose atlieka membranos fiksavimo paviršiuje funkciją, ir sukuria vandeninį sluoksnį, taip atskirdami fosfolipidinį dvisluoksnį nuo kieto paviršiaus. Tokia architektūra leidžia jas pritaikyti baltymų sąveikos su membranomis tyrimams. Šiame darbe, buvo analizuojami trys lipidiniai inkariniai junginiai: WC14, FC16 ir HC18. tBLM suformuotos panaudojant HC18, formuoja dvisluoksnius, pasižyminčius aukšta elektrine varža ir didele lateraline difuzija. Dinaminės fosfolipidų savybės tBLM buvo tirtos fluorescencijos koreliacijos spektroskopijos (FCS) metodą varijuojant inkarinio junginio kiekiu. Buvo pasiūlytas vezikulių liejimosi metodas, įgalinantis pakeisti membranos kompoziciją, kuris remiasi tiesioginiu lipido apsikeitimu tarp vezikulės ir membranos. Šio apsikeitimo egzistavimas ir galimybės pavaizduotos fluorescentiniais metodais, pažymint vezikules fluorescuojančia žyme.

Šiame darbe pavaizduotas, kad α -HL, juodligės toksino ir vaginolizino įsiterpimas į bisluoksnę lipidinę membraną yra tiksliai ir greitai nustatomas EIS metodu, nes toksinų suformuotos poros žymiai padidina tBLM laidumą. α -HL ir PA₆₃ funkcionalumas įrodytas, atliekant osmosinio streso eksperimentą su skirtingos molekulinės masės polimerų tirpalais – polietilenglikoliais (PEG). Buvo nustatyti jonų judėjimo aktyvaciniai barjerai per α -HL ir PA₆₃ poras. Šie rezultatai patvirtino, jog α – hemolizinas ir juodligės toksinas tBLM, kaip ir biologinėse membranose, formuoja vandens pripildytas poras.

Centriniai Alzheimerio ligos patogenezę inicijuojantys biocheminiai junginiai yra viduląsteliniai ir ekstraląsteliniai nedidelės molekulinės masės peptidai – β -amiloidai ($A\beta_{1-42}$), kurie linkę savaimė susiorganizuoti į toksiškus amiloidinius darinius. Šiame darbe tirpūs skirtingo dydžio sintetiniai $A\beta_{1-42}$ oligomerai buvo panaudoti neurotoksiškumo nustatymui ir išsamiam dirbtinių fosfolipidinių bisluoksnų dielektrinio pažeidimo ištyrimui. EIS metodu darbe parodyta, jog $A\beta_{1-42}$ oligomerų sukelti pakitimai yra siejami su membranos dielektrinės konstantos padidėjimu, dėl kurio stipriai išauga membranos laidumas. Rasta, jog membranos sudėtis turi didelę įtaką $A\beta_{1-42}$ oligomerų jungimuisi su fosfolipidinėmis membranomis. Aptikta sąsaja tarp dalelių dydžio ir neurotoksiškumo: didžiausiu toksiškumu pasižymi maži $A\beta_{1-42}$ oligomerai (pagal AFM z aukštį 1 – 3 nm), o tarpu didesnieji (5 – 10 nm, pagal z-aukšti) nebuvo neurotoksiški kultivuojamoms neuronų kultūroms, tačiau antrinė struktūra, nustatyta su FTIR ir CD, nesiskyrė.

CURRICULUM VITAE

Rima Budvytytė

Institute of Biochemistry, Vilnius University, Mokslininku 12, Vilnius. LT- 08662 Tel.: 8-5 2729144 Faks.: 8-5 2729196,
Mobile phone: +37067639590, e-mail: rima.budvytyte@bchi.vu.lt

Place and time of birth: August 18, 1983, Klaipėda, Lithuania.

Education:

2008–2012 PhD studies in Biochemistry, Institute of Biochemistry, Vilnius University Lithuania
2006–2008 Master of Biochemistry, Vilnius University, Lithuania,
2002–2006 Bachelor of Bioengineering, Vilnius Gediminas Technical University, Lithuania

Experience:

Since 2007 Researcher, **Institute of Biochemistry**, Dept. of Bioelectrochemistry and Biospectroscopy.
Summer 2007 Undergraduate Research Fellowship, **Institute of Biochemistry**, Mokslininku 12, LT 08662 Vilnius
Summer 2005 Undergraduate Research Fellowship, **Vilnius University**, Dept. of Biochemistry, Laboratory of Membrane Biochemistry. M.K.Čiurlionio st. 21/27, LT 03101 Vilnius
Summer 2004 Summer Practice, Institute of Biotechnology, Laboratory of Prokaryote Gene Engineering. V. A. Graičiūno st. 8, LT 02241 Vilnius.

Scientific interests:

Investigations of tethered lipid membranes on surface and their interactions with peptides and pore forming toxins with such membranes using electrochemical impedance spectroscopy, fluorescence correlation spectroscopy; Studies of morphology, conformation and toxicity of β -amyloid oligomers as a key molecular components in Alzheimer disease, using atomic force microscopy, dynamic light scattering, circular dichroism and sum frequency generation.

Foreign research visits:

07–09/2006 **National Institute of Standard and Technology**, Biochemical Sciences Division, 100 Bureau Drive, Gaithersburg, MD 20899. USA.
07–09/2009 **Carnegie Mellon University**, Department of Physics, Biological Physics Group. 5000 Forbes ave, Pittsburgh, PA 15213, USA.
12/2009 **Carnegie Mellon University**, Department of Physics, Biological Physics Group. 5000 Forbes ave, Pittsburgh, PA 15213, USA.
07–09/2010 **Carnegie Mellon University**, Department of Physics, Biological Physics Group. 5000 Forbes ave, Pittsburgh, PA 15213, USA.
03 – 04/ 2011 **Carnegie Mellon University**, Department of Physics, Biological Physics group. 5000 Forbes ave, Pittsburgh, PA 15213, USA.
12 /2011 **Université Paris Est Créteil Val-de-Marne**, Institut de Chimie & Matériaux Paris Est, UMR 7182, CNRS, France.

Fellowships:

2010 Graduate Student International Visits Program. The Research Council of Lithuania.
2011 PhD fellowship to scientific visit abroad program. The Research Council of Lithuania.

Awards:

2011 International Travel Award to present an abstract entitled “MEMBRANE AFFINITY AND NEUROTOXICITY OF β -AMYLOID OLIGOMERS” at Biophysical Society 55th Annual Meeting, Baltimore, USA.

2010 Best poster Award at XI International meeting of Lithuanian Biochemical Society, Toliaja, Vilnius.

2009 Master thesis nominated for the best scientific work of young researchers; letter of appreciation by the Lithuanian Science Academy.